
Dynamics of lane distribution flows in freeways

Sofia Samoili, EPFL
Prof. André-Gilles Dumont, EPFL
Prof. Nikolas Geroliminis, EPFL

Conference paper STRC 2013

STRC

13th Swiss Transport Research Conference
Monte Verità / Ascona, April 24-26, 2013

Dynamics of lane distribution flows in freeways

Sofia Samoili
Laboratory of Traffic Facilities
(LAVOC),
Urban Transport Systems
Laboratory (LUTS)
École Polytechnique Fédérale
de Lausanne (EPFL)
GC C1 383, Station 18, 1015,
Lausanne
Phone: +41 21 693 06 02
Fax: +41 21 693 63 49
sofia.samoili@epfl.ch

Prof. André-Gilles Dumont
Laboratory of Traffic Facilities
(LAVOC)
École Polytechnique Fédérale
de Lausanne (EPFL)
GC C1 398, Station 18, 1015,
Lausanne
Phone: +41 21 693 23 89
Fax: +41 21 693 63 49
andre-gilles.dumont@epfl.ch

Prof. Nikolas Geroliminis
Urban Transport Systems
Laboratory (LUTS)
École Polytechnique Fédérale
de Lausanne (EPFL)
GC C2 389, Station 18, 1015,
Lausanne
Phone: +41 21 693 24 81
nikolas.geroliminis@epfl.ch

April 2013

Abstract

Lane density and lane flow distribution are utilised in the current study as characteristics of traffic dynamics for control and planning purposes in freeways with ITS systems. As part of an on-going research, the Lane Flow Distribution Ratio (LFDR) and the Lane Density Distribution Ratio (LDDR) were introduced as main scalability factors for congestion evolution estimation. The preliminary exploratory analysis from LFDR, LDDR, traffic and spatiotemporal parameters along with link fundamental diagrams, indicated dependence between lane vehicle allocation and impending congestion emergence, in terms of traffic levels. This led to a partial parameterisation of driver's behaviour during peak hours, that was studied in several contexts, namely at mainline, on-ramp and off-ramp locations.

The assessment of the developed model was conducted based on observations derived from a freeway site in California. The site is operating during peak hours with high congestion level. Further on this approach, decision thresholds for a number of ITS policies could be derived, to adapt accordingly to control policies (eg. hard shoulder operation, VSL, ramp metering).

Keywords

Lane density distribution – lane flow distribution – hysteresis – congestion evolution

1. Introduction

Traffic dynamics have been extensively analysed through the main macroscopic parameters of flow, density and speed and traffic fundamental diagrams. However, the theoretical definition of Macroscopic Fundamental Diagrams (MFD) (Geroliminis and Daganzo, 2008; Geroliminis and Daganzo, 2007) cannot be globally implemented to every network, as the prerequisite of homogeneous conditions (Daganzo, 2007) within the study site is not invariably satisfied. Furthermore, as the geometrical attributes and the management strategies vary (number of lanes, ramps, existence of VLS, managed lanes etc.), lane-oriented behaviour study could be suggested to delineate the trends (Duret et al. 2012; Chung and Cassidy, 2004; Daganzo, 2002).

The impact of lane distribution at traffic flow near merging zones was observed during several traffic conditions, and patterns independent to the study area geometry and control policy were identified during free-flow regimes (Amin and Banks, 2005; Duret et al., 2012). A lane behavioural model that was established by Daganzo, classifies the drivers into aggressive and less aggressive and denotes that up to congested regimes fast drivers are reluctant to proceed to lane change. However when speed difference becomes marginal, they are dispersing in an attempt to maximize their speed.

Nevertheless, empirical researches acknowledged several regimes and transitional conditions whose traffic patterns could not be sufficiently reproduced by the fundamental diagram, as a high scatter was emerging (Duret et al. 2012; Knoop et al., 2010; Helbing et al., 2009). The origin and magnitude of scatters at MFDs along with the hysteresis phenomenon, which are derived following inconsistent traffic states, were efficiently addressed by aggregating flow and occupancy spatially in low time interval (Geroliminis and Sun, 2011, Ji et al., 2010; Daganzo, 2002). It is noted though that traffic distribution and network characteristics can result to various MFD shapes.

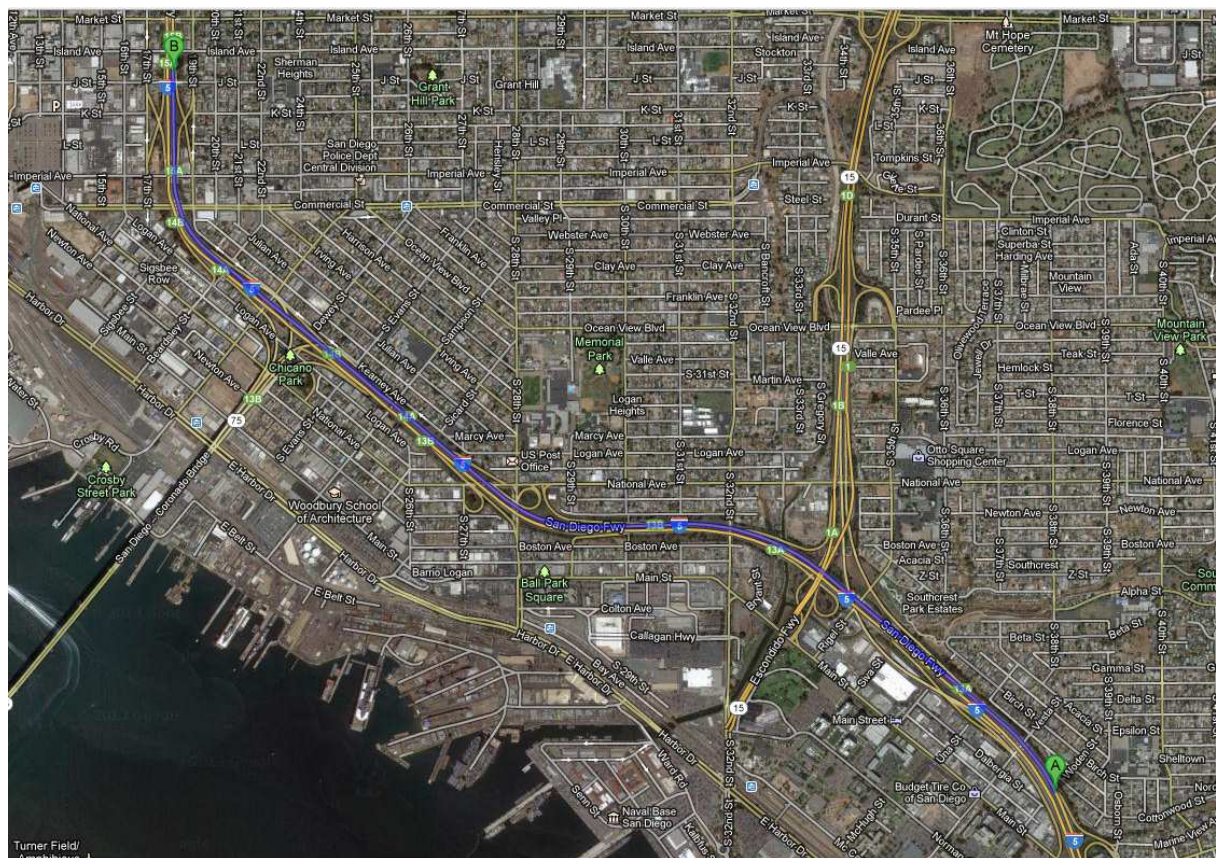
In this paper it is investigated the hypothesis that lane vehicle allocation is influencing traffic regimes expression and hysteretical phenomena in freeways. Based on lane density and flow distributions deductions, traffic patterns are further studied between links with different geometrical attributes and for working days, with time series and flow-density and speed-density relationships. The existence of hysteresis is finally inquired, after a temporal aggregation and conclusions are drawn regarding its cause.

2. Data and Methodology

2.1 Case Study Setup and Data Description

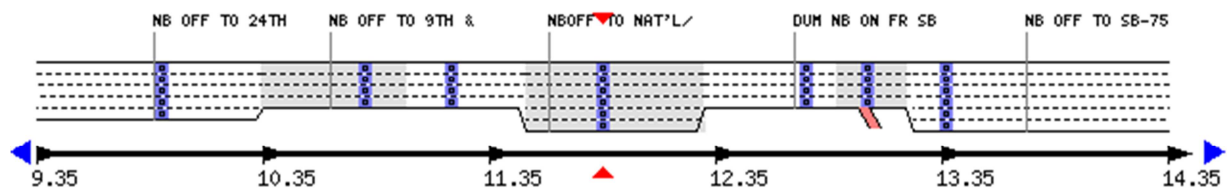
The study site is a 3 miles interstate freeway I5-N with four to six lanes per direction, four off-ramps and one on-ramp, located on district 11 of San Diego County (US). The traffic dataset for this research is consisted of aggregated measurements per $\Delta t=5$ min intervals, collected from four mainline detectors and one off-ramp, which measure flow rate, speed and occupancy per lane, and it is part of the Caltrans Performance Measurement System (PeMS).

Figure 1 a) Study area and b) plan of link of interstate I5-N around detector VDS 1117705, depicted with red triangles. Lane counting starts from the left lane.



Source: maps.google.com

a)



Source: pems.dot.ca.gov

b)

Five links were analysed, four on mainline and one at an off-ramp. Regarding the mainline links, two were selected to have identical topological properties (six lanes without including any on-/off-ramps) and two with a narrower and a wider geometry (4 and 5 lanes), in order to assess a potential impact of topology to the area's traffic dynamics.

2.2 Methodology

2.2.1 Locally Weighted Regression

In order to explore the traffic behaviour, locally weighted regression, or hereinafter loess, was employed. Loess was introduced by Cleveland (Cleveland, 1978) as a memory-based non-parametric regression that fits a regression surface to data through a multivariate smoothing. In recent studies it is implied that that loess outperforms nearest-neighbourhood and kernel smoothing and that in dynamic traffic assignment systems (DTA) with traffic dynamics model, speed estimation accuracy is improved (Cleveland & Devlin, 1988; Sun et al., 2003; Antoniou and Koutsopoulos, 2006; Toledo and Koutsopoulos, 2007). Following the analytical mathematical background of loess in Cleveland and Devlin (Cleveland & Devlin, 1988), the values of the response variable, with y_i measurements, are smoothed as a function of the explanatory, p variables with x_i measurements (for $i = 1, \dots, n$). The response variable is estimated around a "seed" point of a local subset, repeatedly shifting forward to the next point of the original dataset. The predicted data are computed by $y_i = \hat{g}(x_i) + \varepsilon_i$, where $\hat{g}(x_i)$ represents the estimate of the regression surface over a local surface around each value x_i in the p -dimensional space of the independent variables, and ε_i the residual errors. The estimate $\hat{g}(x_i)$ at x_i uses the q number of observations (in range $1 < q \leq n$, for q integer) whose x_i distance is closer to x . According to this distance, a weight in the form of the tricube function is computed (eq. 1):

$$W(u) \equiv \begin{cases} (1 - u^3)^3, & \text{if } 0 \leq u < 1 \\ 0 & \text{otherwise} \end{cases} \quad (1)$$

where u is the space mean speed. The weight is allocated to each point (y_i, x_i) , so that the weight function is (eq. 2):

$$w_i(x) = W\left(\frac{\rho(x, x_i)}{d(x)}\right) \quad (2)$$

whose range varies from 0 for the q th-nearest x_i to x , increasing as the x_i is closer to x . The $\rho(x, x_i)$ is the distance function running in the space of independent variables and $d(x)$ is the distance of the q th-nearest x_i to x . The fitting and prediction procedure is completed when the objective function, namely the weighted residual sum of squares, is minimised (eq. 4) (Antoniou and Koutsopoulos, 2006):

$$\min J(\sum_{i=1}^n w_i \epsilon^2) \quad (3)$$

2.2.2 Moving Average

To smooth any rapid fluctuations that can occur at freeways, so as to not interfere with the interpretation of the expression of traffic stream dynamics and to identify the reasons behind any alterations of the trend, a simple moving average (SMA) was employed. In this regard, the dataset was analysed based on series of averages of a fixed subset of 5-min calculated for a fixed period of 15-min.

Given a sequence of density $\{k_i\}_{i=1}^N$, flow $\{Q_i\}_{i=1}^N$ and speed $\{V_i\}_{i=1}^N$, the n -moving average are respectively the new sequences $\{s_{k_i}\}_{i=1}^{N-n+1}$, $\{s_{Q_i}\}_{i=1}^{N-n+1}$, $\{s_{V_i}\}_{i=1}^{N-n+1}$ defined from the k_i , Q_i , V_i by computing the arithmetic mean of subsequences of n terms: $s_{k_i} = \frac{1}{n} \sum_{j=i}^{i+n-1} a_j$, $s_{Q_i} = \frac{1}{n} \sum_{j=i}^{i+n-1} a_j$, $s_{V_i} = \frac{1}{n} \sum_{j=i}^{i+n-1} a_j$ (Kenney and Keeping, 1962).

3. Exploratory Analysis of Traffic Dynamics

For an insight in the traffic dynamics of freeways and congestion evolution estimation, lane density distribution ratio (LDDR) and lane flow distribution ratio (LFDR) are introduced in the current research. Furthermore, time series of traffic parameters, namely density, flow rate and speed, and link fundamental diagrams were studied, to define the factors that lead to congestion emergence during a period a one week (01-05/11/2010).

The LFDR and LDDR during morning peak hours per weekday per direction are presented in Figures A1 and A2, comparing multiple detectors at mainline and one at an off-ramp. The ratio of flow or density of each lane, divided by the total flow or density of the direction is plotted at axis Y, and the total density per direction at X. The relationship that relates the ratios of each lane can be described as follows (eq.4):

$$a_i \cdot r_{Q_i} + \beta = a_i \cdot \frac{Q_i}{Q_{dir}} + \beta = 1 \quad \text{or} \quad a_i \cdot r_{k_i} + \beta = a_i \cdot \frac{k_i}{k_{dir}} + \beta = 1 \quad (4)$$

$$\text{for } Q_{dir} = \sum_i Q_i \in \mathbb{R} \setminus \{0\} \quad \text{and} \quad k_{dir} = \sum_i k_i \in \mathbb{R} \setminus \{0\}$$

where i is denoting the left, right or median lanes, r_i is ratio of the lane flow (LFDR) or density distribution (LDDR) per lane (hereinafter expressed in percentage) over the total density per direction, k_i the density per lane, k_{dir} the total density per direction, computed by the per lane density constrained by 0 (as it is appointed as the divisor of the k_i), and a_i , β the coefficients that are estimated by loess (Samoili et al., 2013).

The data were fitted per day and per lane with loess models, in order to attain a more accurate overview. For free-flow conditions, where total density is approximately lower than 80 veh/mile, users prefer the median lanes next to the right lane (median 4 and 5 in the figure), as they are depicted to carry respectively $r_{k_{m4}} \cong 23\%$ and $r_{k_{m3}} \cong 22\%$ of the total density, as well as the median lane next to the left lane (median 1) that carries $r_{k_{m1}} \cong 20\%$. In denser regimes ($k_{dir} \cong 115$ veh/mile), there is an approximately 5% increase of the left lane users ($r_{k_{mL}} \cong 20\%$) and a borderline increase of the right lane volume, potentially depicting the reception of the first and third median lanes that are mutually decreasing ($r_{k_{m1}} \cong 20\%$ and $r_{k_{m3}} \cong 16\%$). Shortly before the maximum capacity of the link is attained, the main volume is still attracted by the median lanes, and only when congested regimes are prevailing in every lane, flow is distributing to the right lane. Consequently, in jammed flow conditions ($k_{dir} > 130$ veh/mile) the significantly greater density of the right lane, as it is revealed from the LDDR, is suggesting that the users of the remaining lanes pass to the right lane only when the geometry of the link is more favourable, namely when more lanes are present, or in the area of a junction, that is before an off-ramp or after an on-ramp.

The heterogeneity of driving behaviour between lanes, and thus the differentiation of maneuvering and its effects on traffic states emergence for every link, was further inquired with the employment of time series of flow, density and speed. Apart from the expected variation of traffic patterns per day, a delay in the harmonization of density and flow within the same link and at the links downstream is observed. This indicates that a bound or congested flow upstream causes the occurrence of the respective traffic states in the successive links. For example, in the time series of flows and densities, where the black points represent respectively the flow and density per direction per 5-min intervals (Figure A3), on Wednesday the capacity drop happens after the maximum capacity is reached at 7:35 am for approximately $Q_{dir} \cong 11'000$ veh/mile (Figure A3 a1), which affects the link downstream (Figure A3 b1) with a 5 minutes lag and persists until the end of the study area (Figure A3 e1). The bound and congested flow states that are identified in both time and space with the time series of flows for every link, are distinctively encountered also by those of density, within which the maximum density occurs shortly after the maximum capacity of the link is expressed. In addition, it was observed that even though the congestion is propagating downstream, the magnitude of congestion is different between links of comparable geometrical attributes.

To further investigate these dynamics, fundamental diagrams of flow-density were studied for five weekdays (01-05/05/2010), in two aggregation levels, per lane and per direction, fitted by locally weighted regression (loess) for a more immediate overview (Figure A4 a1-e1, a2-e2 respectively). As it is shown i.e. in Figure A4 a1 in the left and first median lane, scatters are formed for values of density ($k_l \cong 40$ veh/mile) that maximize flow ($Q_l \cong 2200$ veh/h) for every day except Monday. In Figure A4 a2 that all the lanes are aggregated per direction, the formation of scatters is presented smoother or even masked for Friday and Wednesday. The hysteresis phenomenon is more pronounced at the off-ramp (Figure A4 c1, c2) and for links with wider geometry (Figure A4 a, d, e).

Based on the idea of Geroliminis et al. (Geroliminis and Sun, 2011; Geroliminis and Daganzo, 2008) to spatially aggregate flow and occupancy, so as to examine the non-existence of well-defined MFD's for hysteretical freeway networks, a temporal aggregation of density and flow with a moving average of a 5-min interval every 15-min was conducted. The aggregation smoothed the rapid fluctuations of these parameters that result to capacity drop, nevertheless hysteresis persisted, as it is depicted in Figures A3 and A5, where the black points represent the observed values, and the coloured the values that resulted by the aforementioned moving average window in levels of speed. The flow-density diagrams illustrate high scatters for high values of density that maximize flow, even if the level of density varies across the links. For example in figure A5 a, hysteresis loops are expressed even after the aggregation at the mainline $k_{dir} > 150$ veh/mile for levels of speed of $V_{dir} \cong 60$ miles/h, but also at the off-ramp at $k_{dir} > 125$ veh/mile for $V_{dir} \cong 50$ mile/h (Figure A5 c).

4. Conclusions and Perspectives

In order to provide a timely management of recurrent congestion emergence in freeways, the anticipation and magnitude of capacity drop could mitigate the congestion effects, in terms of travel times and delays. In that scope, a study of traffic dynamics was required, mainly in lanes' level of scale. The preliminary exploratory analysis that employed LFDR, LDDR, traffic and spatiotemporal parameters, as well as link fundamental diagrams, indicated dependence between lane vehicle allocation and impending congestion emergence. The LFDR and LDDR diagrams were studied to inquire the lanes' heterogeneity of flow and density, which can consist one of the reasons of the scatters at the flow-density fundamental diagrams. The spatial and temporal identification of traffic states delineated through time series of speed and density. Moreover, indications of hysteresis emerged, imposing a thorough examination through flow-density relationships. The comparative analysis between the time series and the fundamental diagrams in two spatial aggregation levels, per lane and per direction, confirmed the existence of hysteresis. The moving average implementation on flow, density and speed empirical data, smoothed the rapid fluctuations that commonly appear in freeways, although persisting hysteretical phenomena were conceded.

From the study of the LDDR and LFDR relationships, it was observed that during free flow conditions users prefer the median lanes next to the right lane. As vehicles enter denser regimes, volume increase of the left lane and of the left median lanes follows, along with a mutual decrease of the right median lanes. The middle median lanes appear to be the least preferred, and to serve mainly as a passing lane. Before maximum link capacity is reached, it is revealed that regardless the fact that near free flow conditions prevail in the right lane and the right median lanes, vehicles are in dense regimes at left and left median lanes and these lanes' density is persistently ascending until the capacity drop. Only when jammed density occurs, users pass to the right lane.

Density-flow fundamental diagrams and time series analysis of the main traffic parameters endorsed the induction that right median lanes and the right lane are occupied by slow drivers. Even though free flow speeds are attained in the latter, the other lanes demonstrate higher speed levels and dense regimes, rendering the rightmost lanes under-utilised, potentially due to the fast drivers' attempt to not be bounded by slower-moving vehicles. Middle and leftmost median lanes may also be mainly occupied, as a prevention of drivers to proceed to excessive lane-changing. Furthermore, it is denoted that when traffic conditions are near free flow, but maximum link capacity is approached, a moderate increase of flow rate can rapidly evoke the emergence of denser regimes. Howbeit, when this link is near its minimum capacity, only significant disturbances during free flow conditions can lead to bound flow.

The existence of hysteresis phenomena that were inducted in the time series, were confirmed with density-flow diagrams, mainly at mainline links with wider geometry and at off-ramps. Although an aggregation was followed to reduce any rapid variations of flow that would result in transient conclusions, the hysteresis loops were preserved, sustained presumably by the consistent vehicle allocation in lanes.

Forthcoming research is envisaged with spatial and various temporal aggregations, in several types of freeway networks, equipped or not with ITS policies (i.e. managed lane freeways, VSL, ramp metering etc.), so as to determine the reasons that lay behind the stated phenomena under recurrent congested regimes.

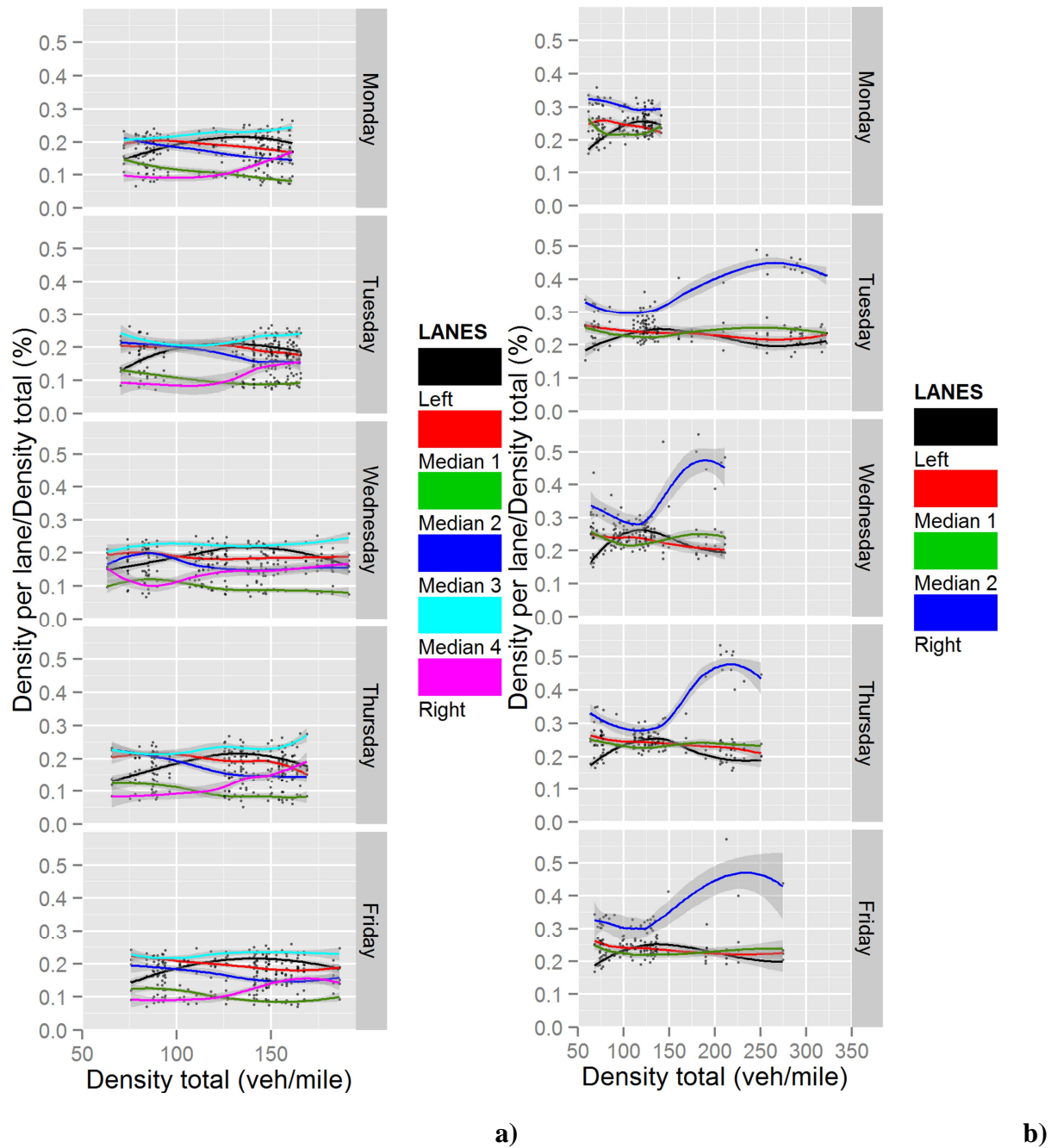
5. References

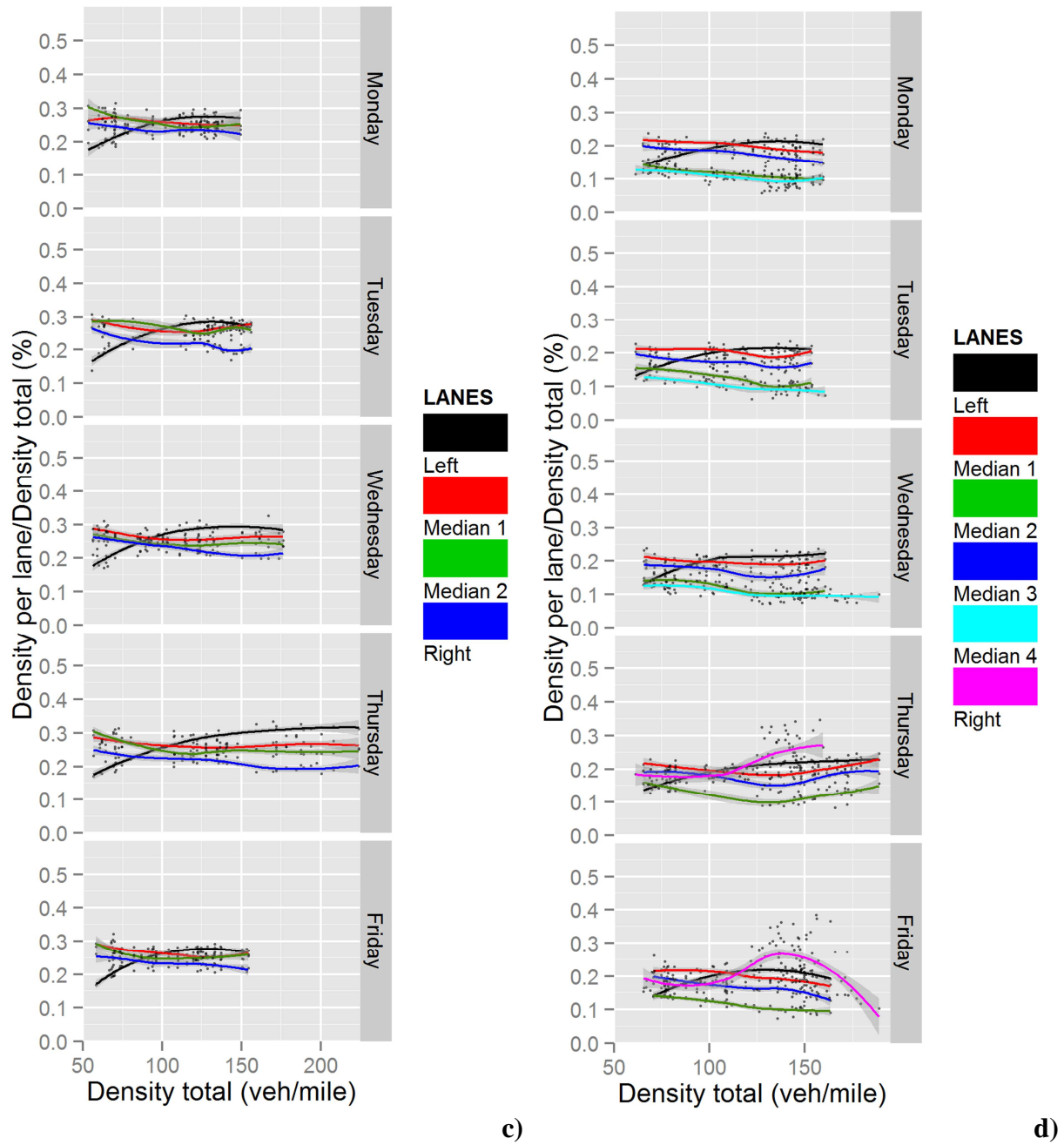
- Antoniou, C. and H. Koutsopoulos. Estimation of Traffic Dynamics Models with Machine Learning Methods, In *Transportation Research Record: Journal of the Transportation Research Board*, No. **1965**, Transportation Research Board of the National Academies, Washington, D.C., pp. 103 – 111.
- Amin, M. R. and J. H. Banks (2005). Variation in freeway lane flow patterns with volume, time of day, and location, In *Transportation Research Record: Journal of the Transportation Research Board*, No. **1934**, Transportation Research Board of the National Academies, Washington, D.C., pp.132–139.
- Chung, K. and M. J. Cassidy (2004). Test of theory of driver behavior on homogeneous freeways. In *Transportation Research Record: Journal of the Transportation Research Board* No. **1883**, Transportation Research Board of the National Academies, Washington, D.C., pp. 14–20.
- Cleveland, W. S., and S. J. Devlin (1988). Locally Weighted Regression: An Approach to Regression Analysis by Local Fitting. *Journal of the American Statistical Association*, Vol. **83**, pp. 596–610.
- Cleveland, W. S (1978). Robust Locally Weighted Regression and Smoothing Scatterplots. *Journal of the American Statistical Association*, Vol. **74**, pp. 829–836.
- Daganzo, C. F. (2007). Urban Gridlock: Macroscopic Modeling and Mitigation Approaches. *Transportation Research Part B*, Vol. **41** (1), pp. 49–62.
- Daganzo, C.F. (2002). A behavioral theory of multi-lane traffic flow. Part I: long homogeneous freeway sections. *Transportation Research Part B*, Vol. **36** (2), pp 131–158.
- Duret, A., S. Ahn, and C. Buisson (2012). Lane Flow Distribution on a three-lane freeway: General features and the effects of traffic controls. *Transportation Research Part C: Emerging Technologies*. Vol. **24**, pp. 157-167.
- Geroliminis, N. and Sun, J. (2011). Hysteresis phenomena of a macroscopic fundamental diagram in freeway networks. *Transportation Research Part A: Policy and Practice*, **45**(9), pp. 966–979.
- Geroliminis, N. and Daganzo, C.F. (2008). Existence of urban-scale macroscopic fundamental diagrams: some experimental findings. *Transportation Research Part B*, **42**(9), pp.759–770.
- Geroliminis, N., and C. F. Daganzo (2007). Macroscopic Modeling of Traffic in Cities. Presented at *86th Annual Meeting of the Transportation Research Board*, Washington, D.C.
- Helbing, D., Treiber, M., Kesting, A. and M., Schönhof (2009). Theoretical vs. empirical classification and prediction of congested traffic states. *European Physical Journal B*, **69** (4), pp.583–598.

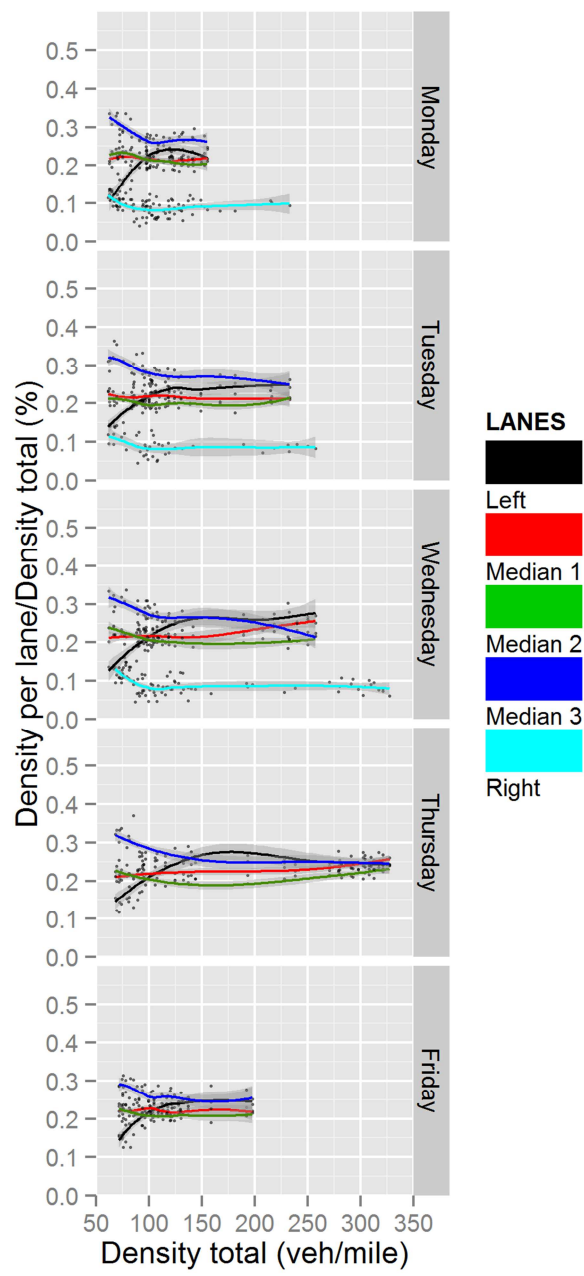
-
- Ji, Y., Daamen, W., Hoogendoorn, S., Hoogendoorn, Lanser, S., and X. Qian (2010). Macroscopic fundamental diagram: Investigating its shape using simulation data. *Transportation Research Record*, **2161**, pp. 42–48.
- Kenney, J. F. and Keeping, E. S. (1962). The k-Statistics, *Mathematics of Statistics*, Pt. 1, 3rd ed. Princeton, NJ: Van Nostrand, pp. 99-100.
- Knoop, V.L., Duret, A., Buisson, C., and Van Arem, B. (2010). Lane Distribution of Traffic Near Merging Zones - Influence of Variable Speed Limits , *Proceedings of the IEEE conference on Intelligent Transport Solutions*, Madeira, Portugal, September 2010.
- Toledo, T., Koutsopoulos, H. N. and K. Ahmed (2007). Estimation of Vehicle Trajectories with Locally Weighted Regression. In *Transportation Research Record: Journal of the Transportation Research Board*, No. **1999**, Transportation Research Board of the National Academies, Washington, D.C., pp. 161-169.
- Samoili S., D. Efthymiou, C. Antoniou and A.-G. Dumont (2013). Lane flow distribution investigation of hard shoulder running freeways. *Transportation Research Record: Journal of the Transportation Research Board* (accepted for publication).
- Sun, H., Liu, H., Xiao, H., He, R., and B. Ran (2003). Use of local linear regression model for short term traffic forecasting, *Transportation Research Record: Journal of the Transportation Research Board*, No. **1836**, Transportation Research Board of the National Academies, Washington, D.C.

Annexes

Figure A1 Diagrams of lane density distribution ratio (LDDR) for 5-min aggregated data during morning peak hours (6:30 – 9:55) per weekday (01-05/11/2010), fitted with loess for (in order from upstream to downstream): a) detector VDS 1117705 at mainline, 6 lanes, b) detector VDS 1114211 at mainline, 4 lanes, c) detector VDS 1117762 at off-ramp, 4 lanes, d) detector VDS 1114219 at mainline, 6 lanes and e) detector VDS 1117782 at mainline, 5 lanes.







e)

Figure A2 Diagrams of lane flow distribution ratio (LFDR) for 5-min aggregated data during morning peak hours (6:30 – 9:55) per weekday (01-05/11/2010), fitted with loess for (in order from upstream to downstream): a) detector VDS 1117705 at mainline, 6 lanes, b) detector VDS 1114211 at mainline, 4 lanes, c) detector VDS 1117762 at off-ramp, 4 lanes, d) detector VDS 1114219 at mainline, 6 lanes and e) detector VDS 1117782 at mainline, 5 lanes.

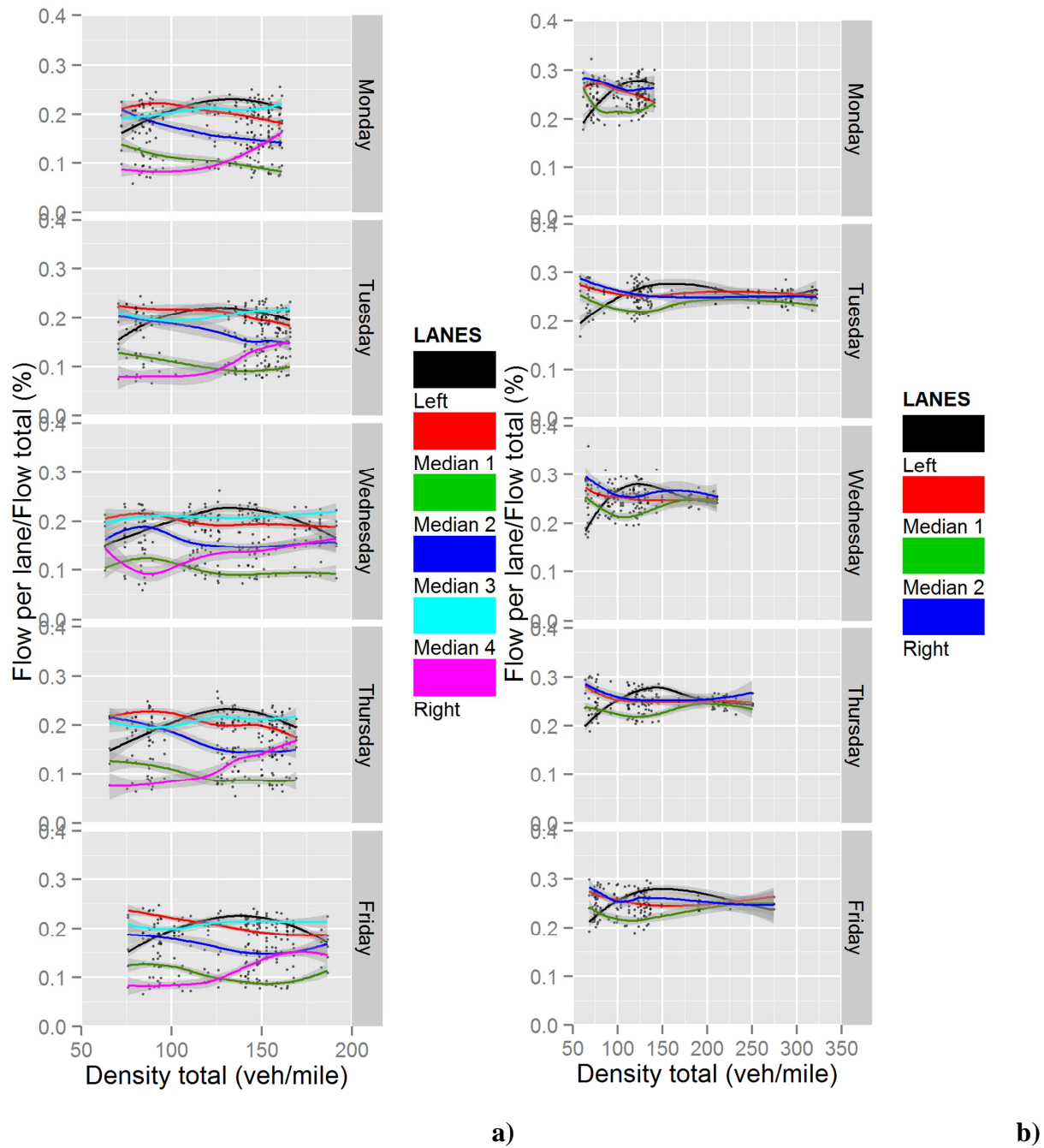
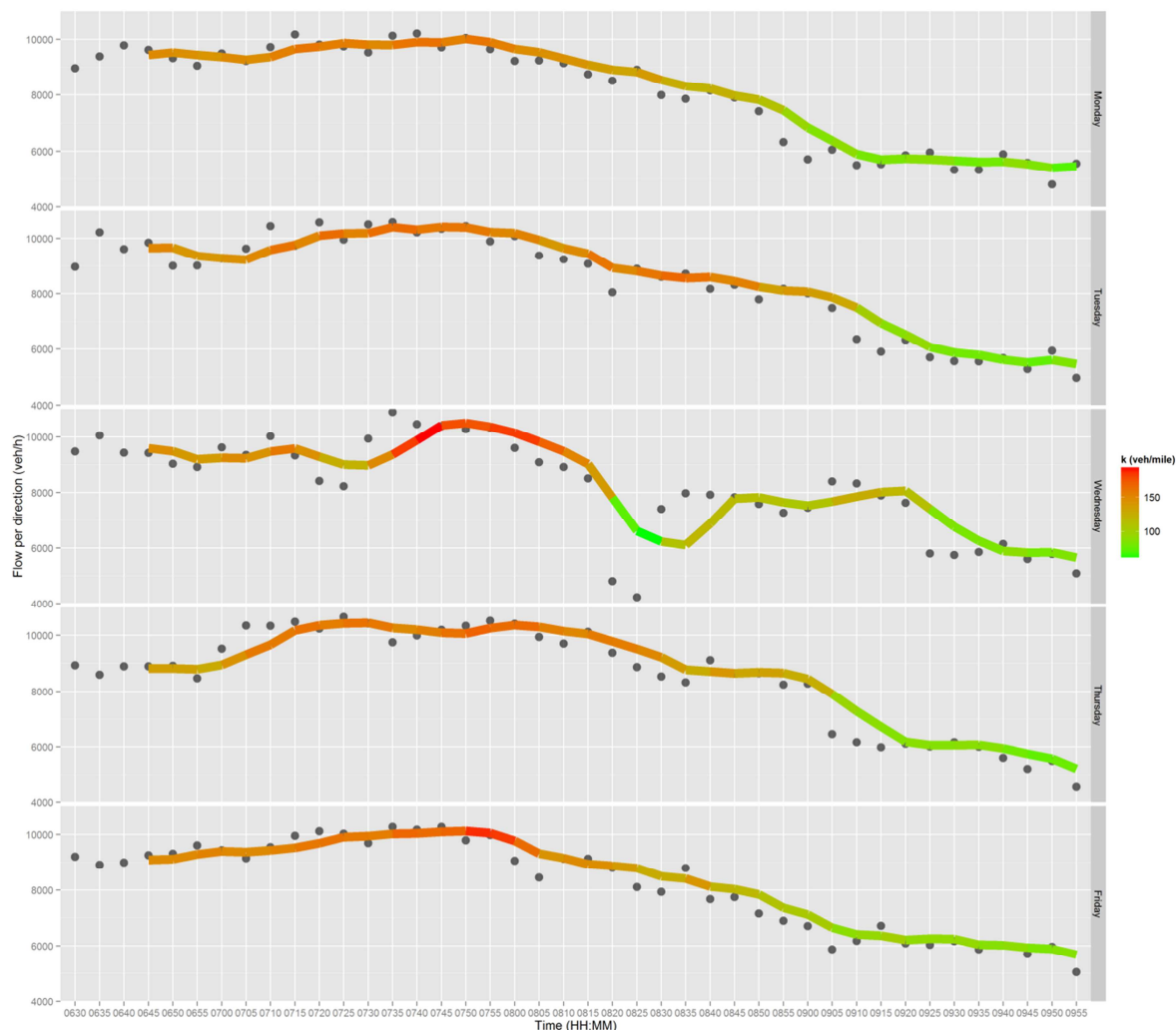
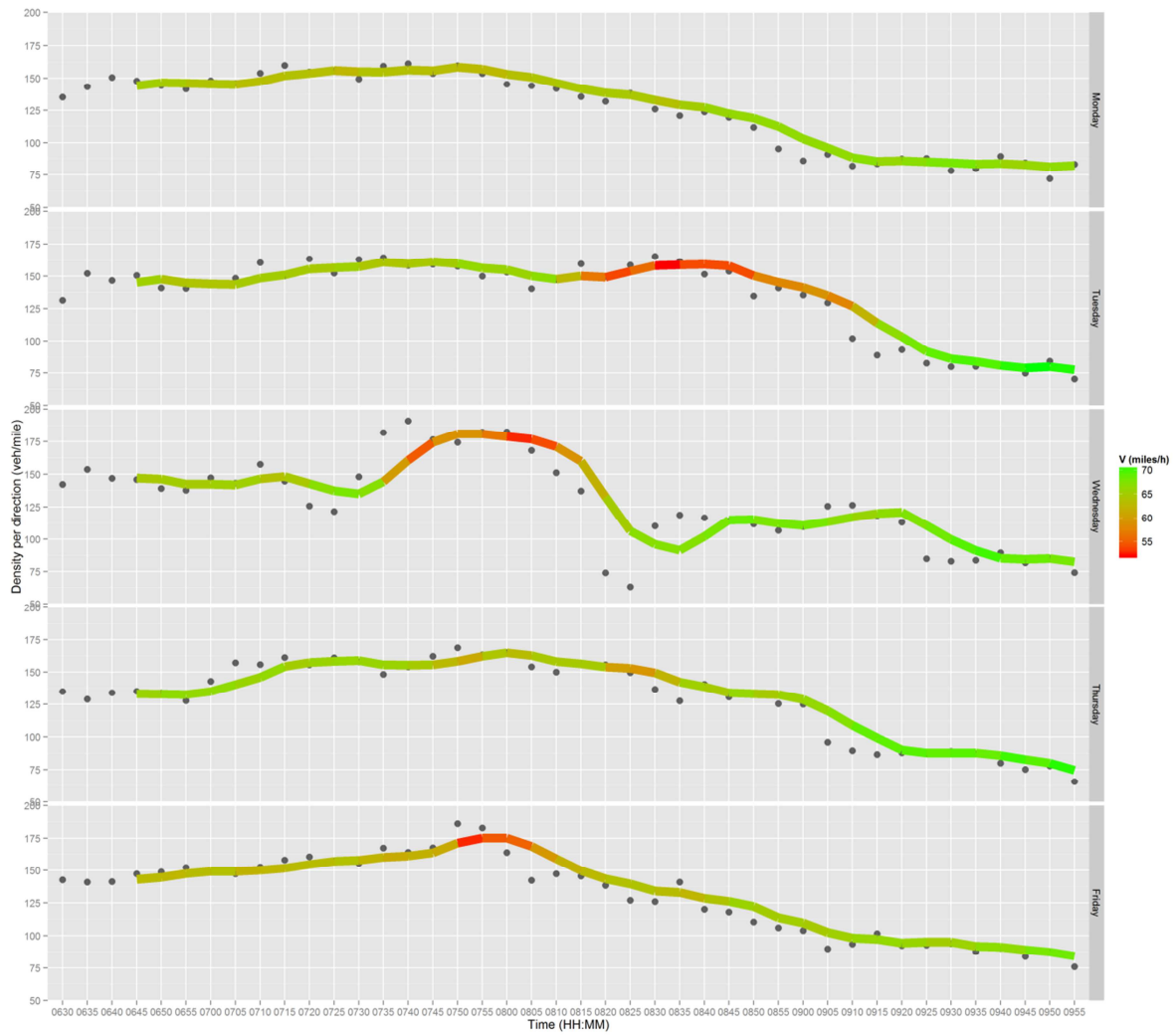


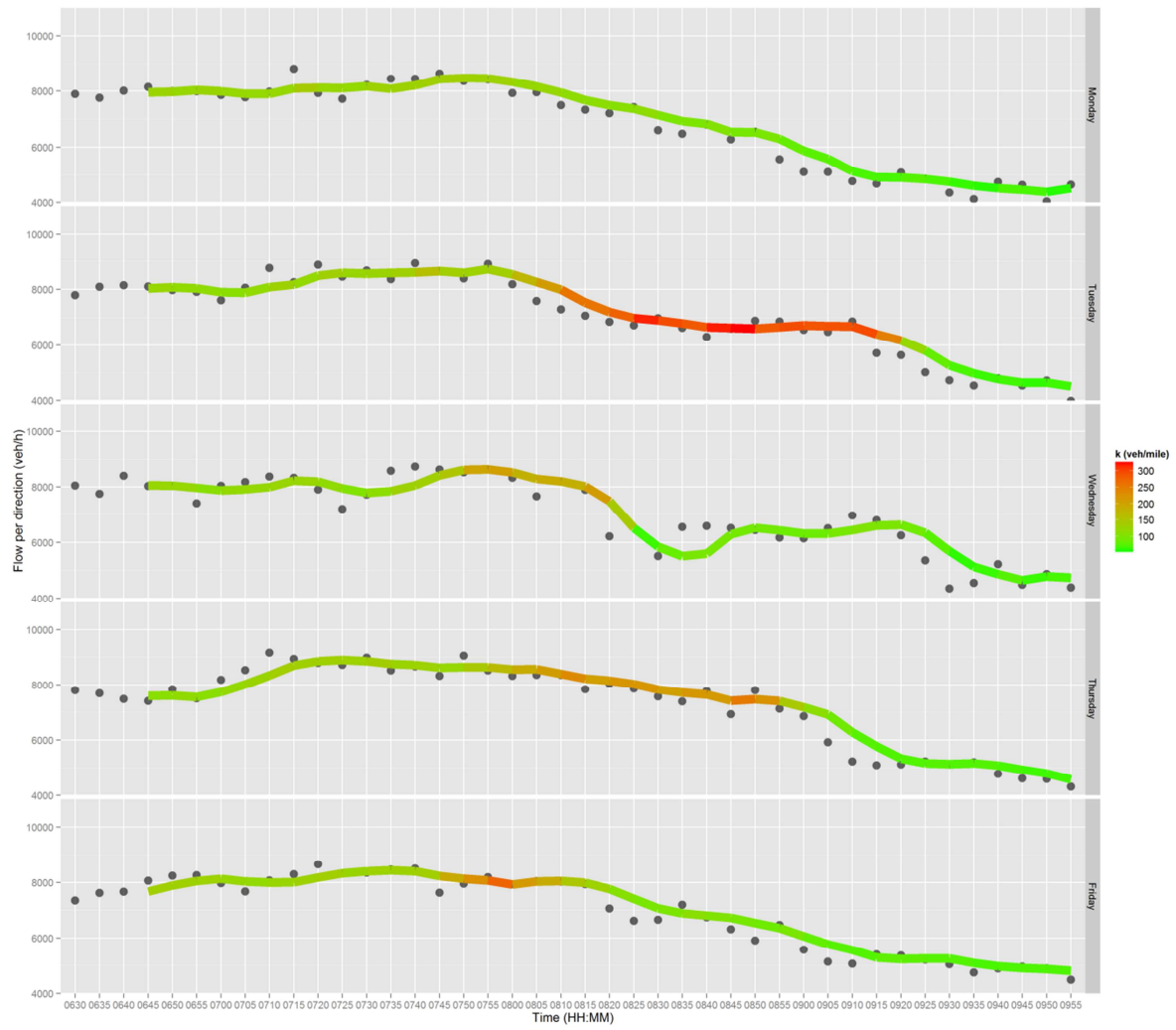
Figure A3 Time series of flow (plots with index 1) and density (plots with index 2) for 5-min aggregated data during morning peak hours (6:30 – 9:55) per weekday (01-05/11/2010), fitted with loess for (in order from upstream to downstream): a) detector VDS 1117705 at mainline, 6 lanes, b) detector VDS 1114211 at mainline, 4 lanes, c) detector VDS 1117762 at off-ramp, 4 lanes, d) detector VDS 1114219 at mainline, 6 lanes and e) detector VDS 1117782 at mainline, 5 lanes. With black points are depicted the observed values of flow and density, with lines the values of these parameters as result of a 5-min moving average every 15-min. In colour are plotted the values of density and speed (plots of index 1 and 2 respectively) as result of a 5-min moving average every 15-min.



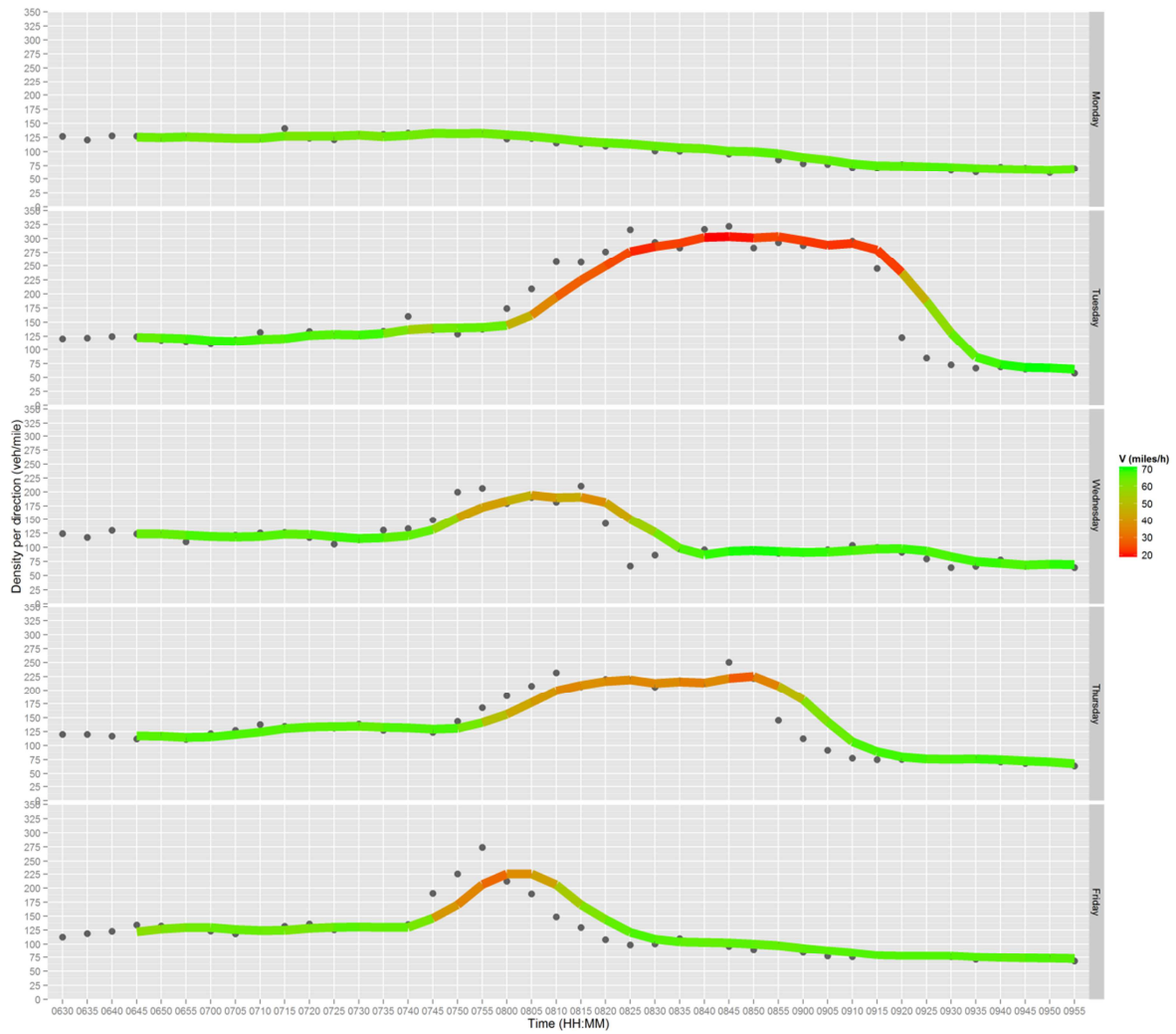
a1)



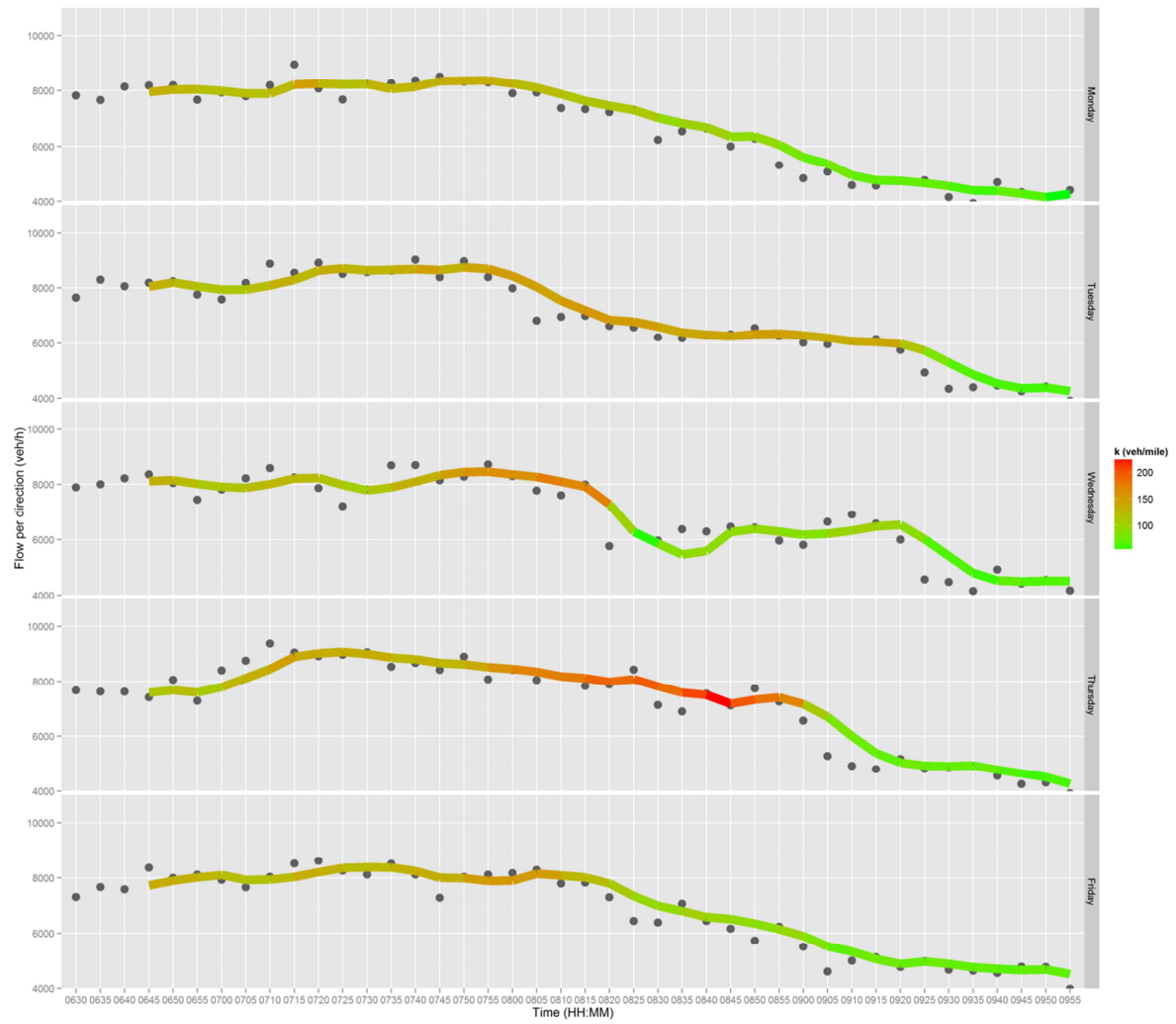
a2)



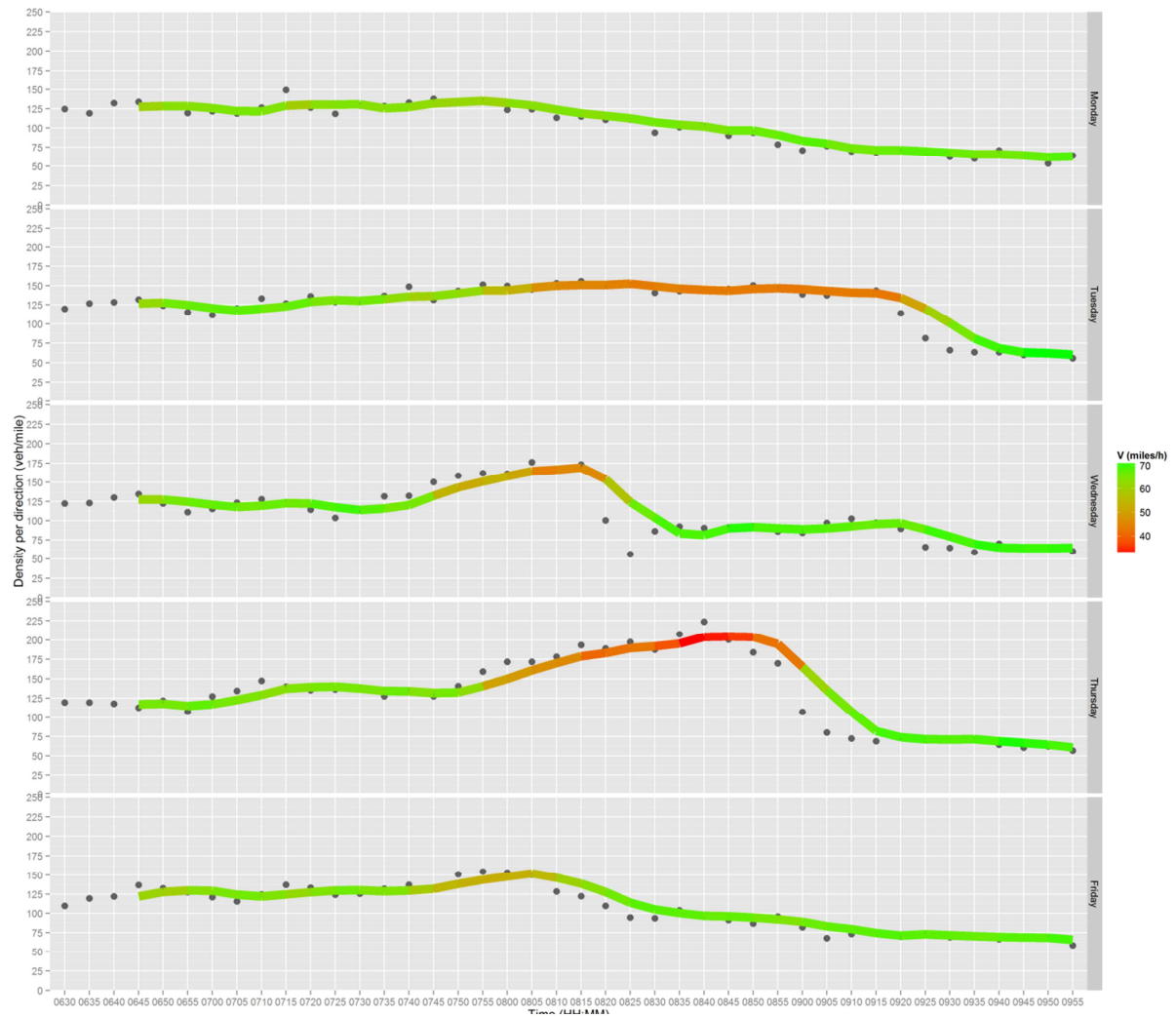
b1)



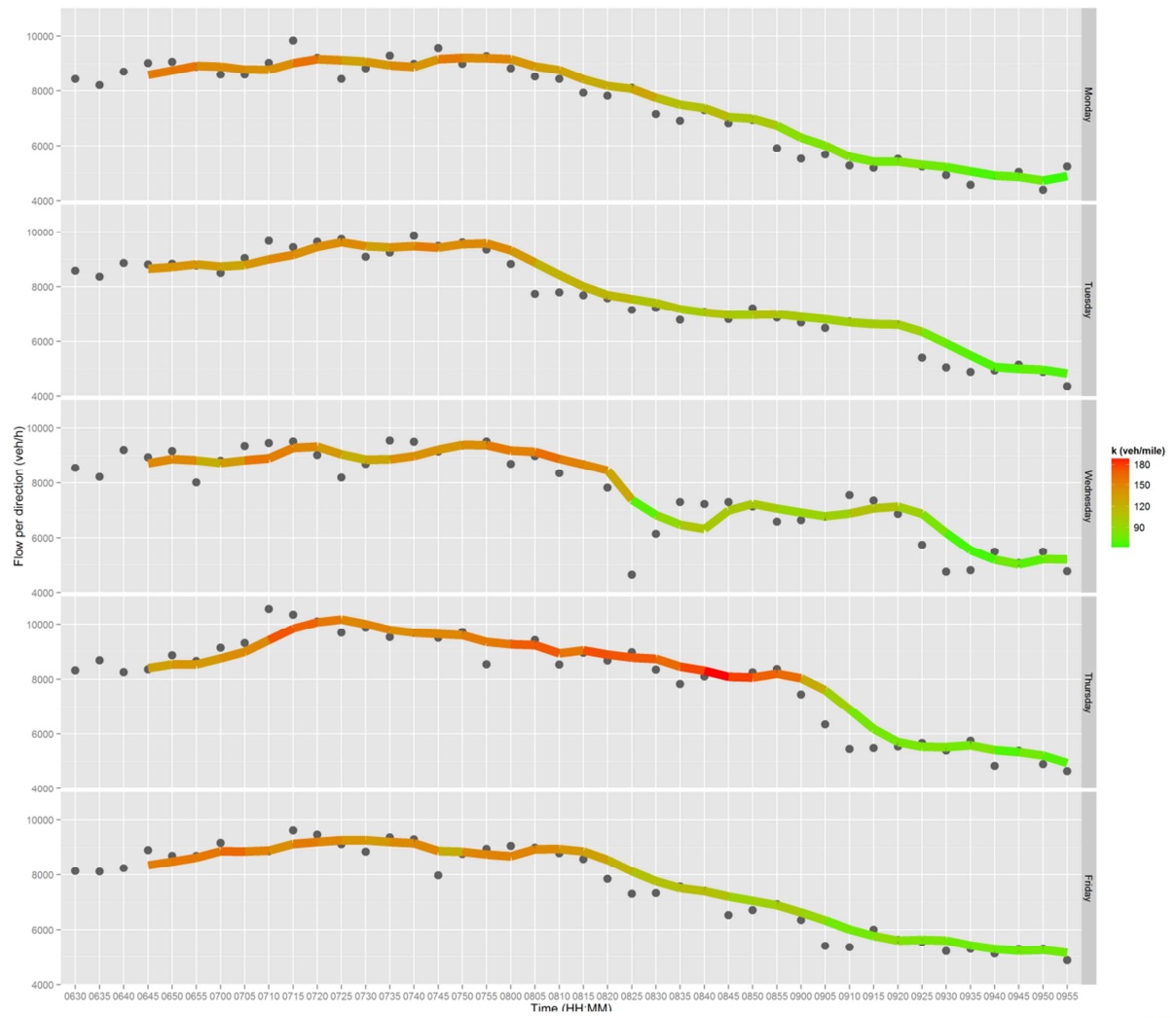
b2



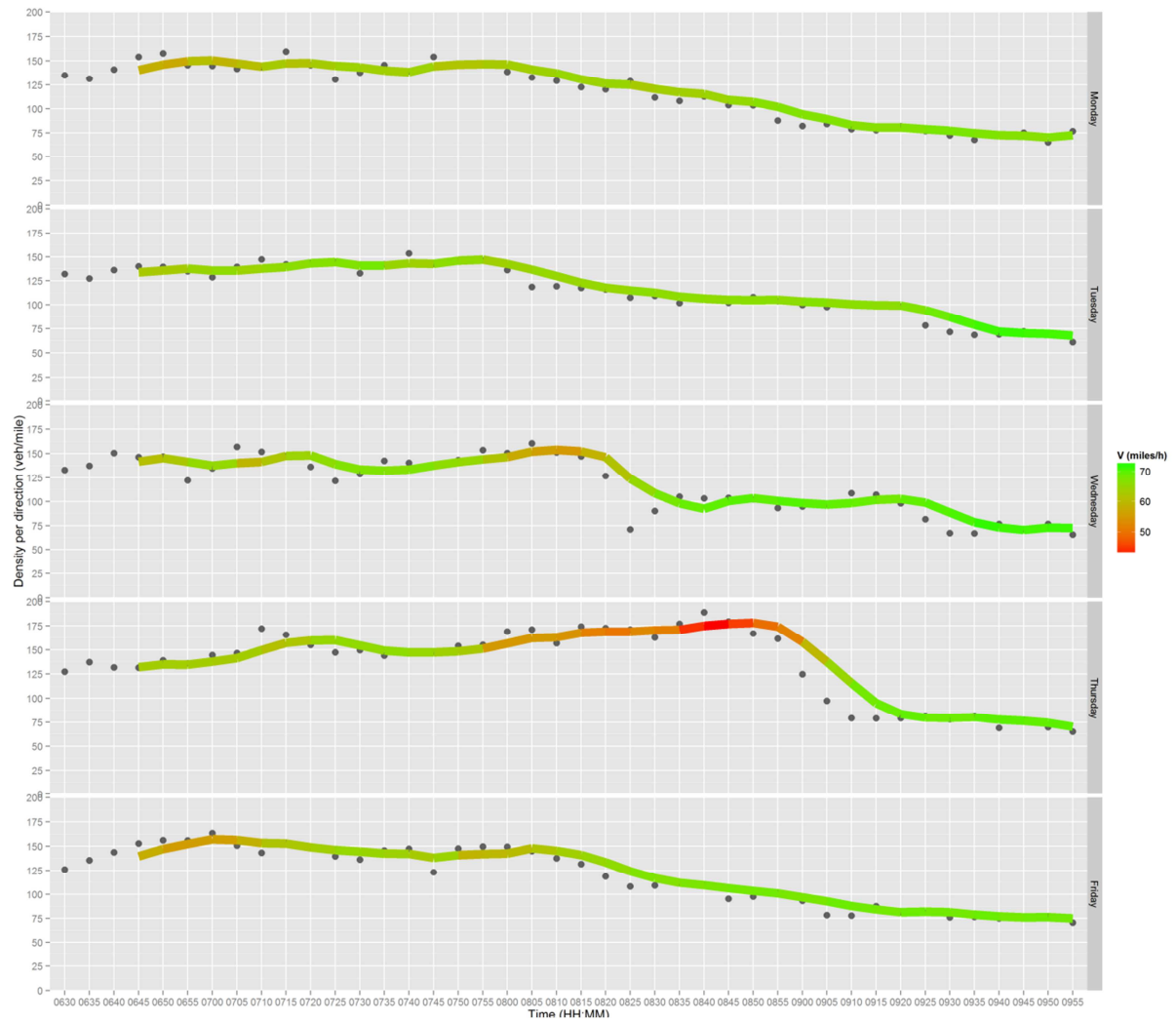
c1)



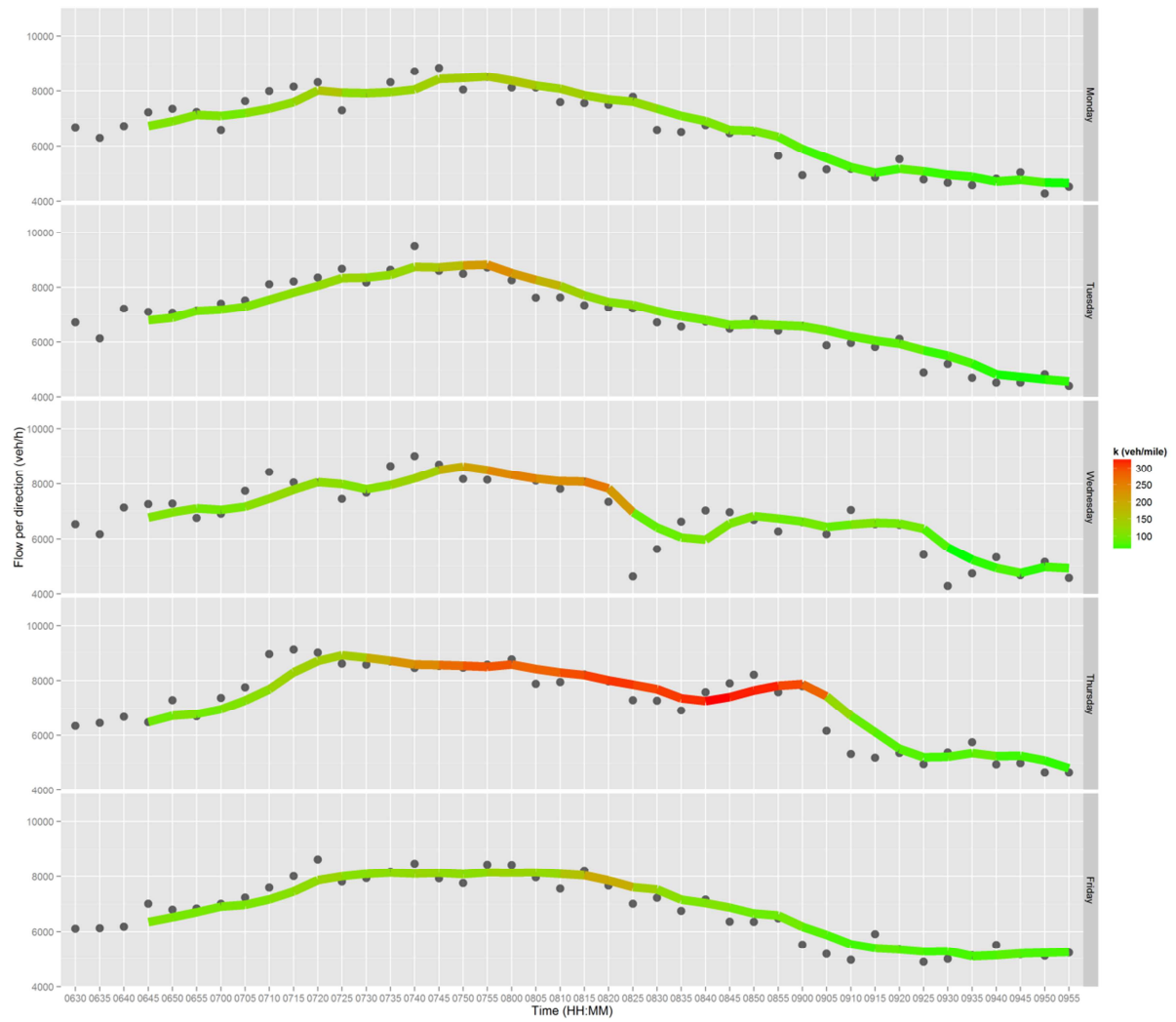
c2)



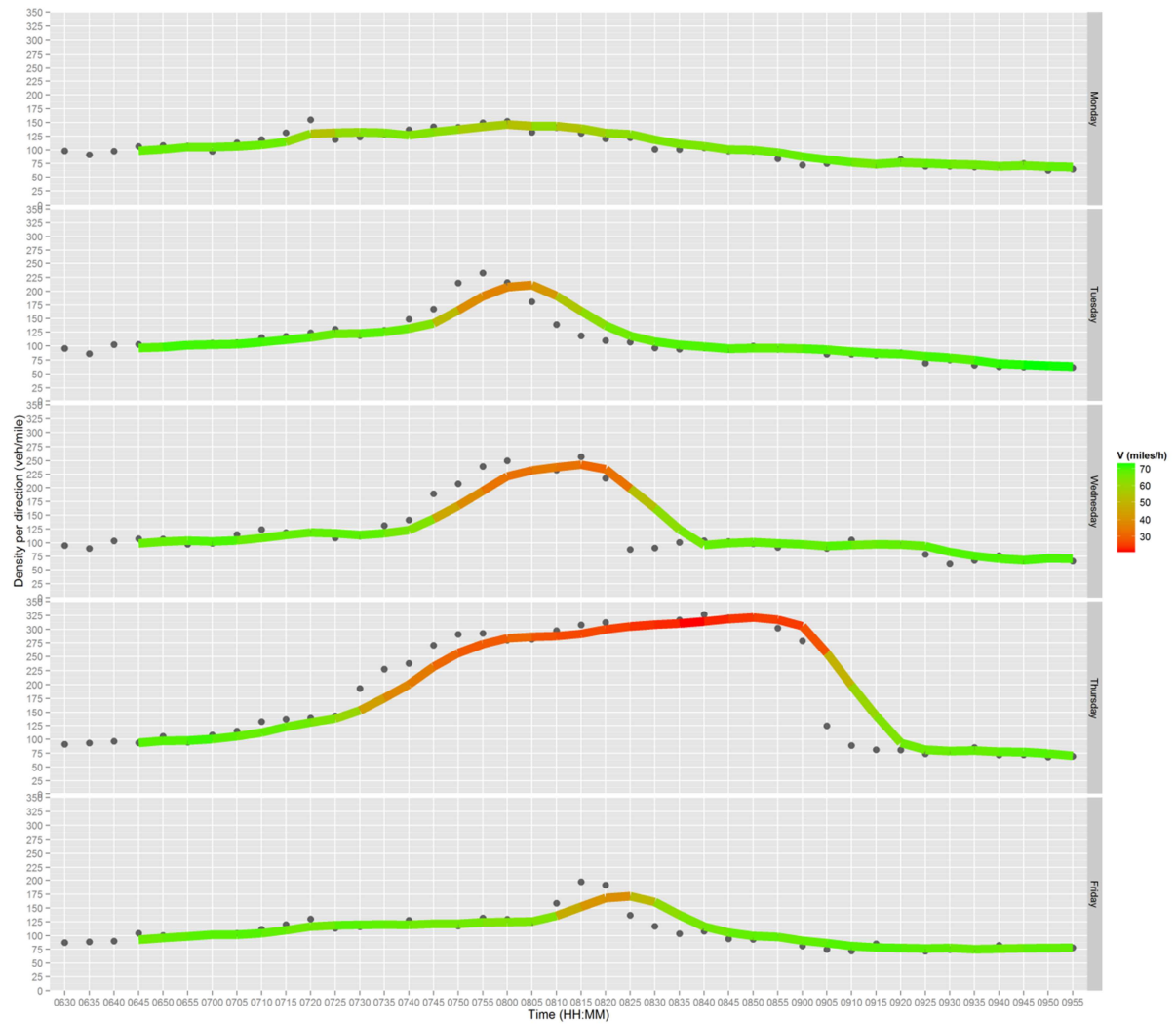
d1)



d2)

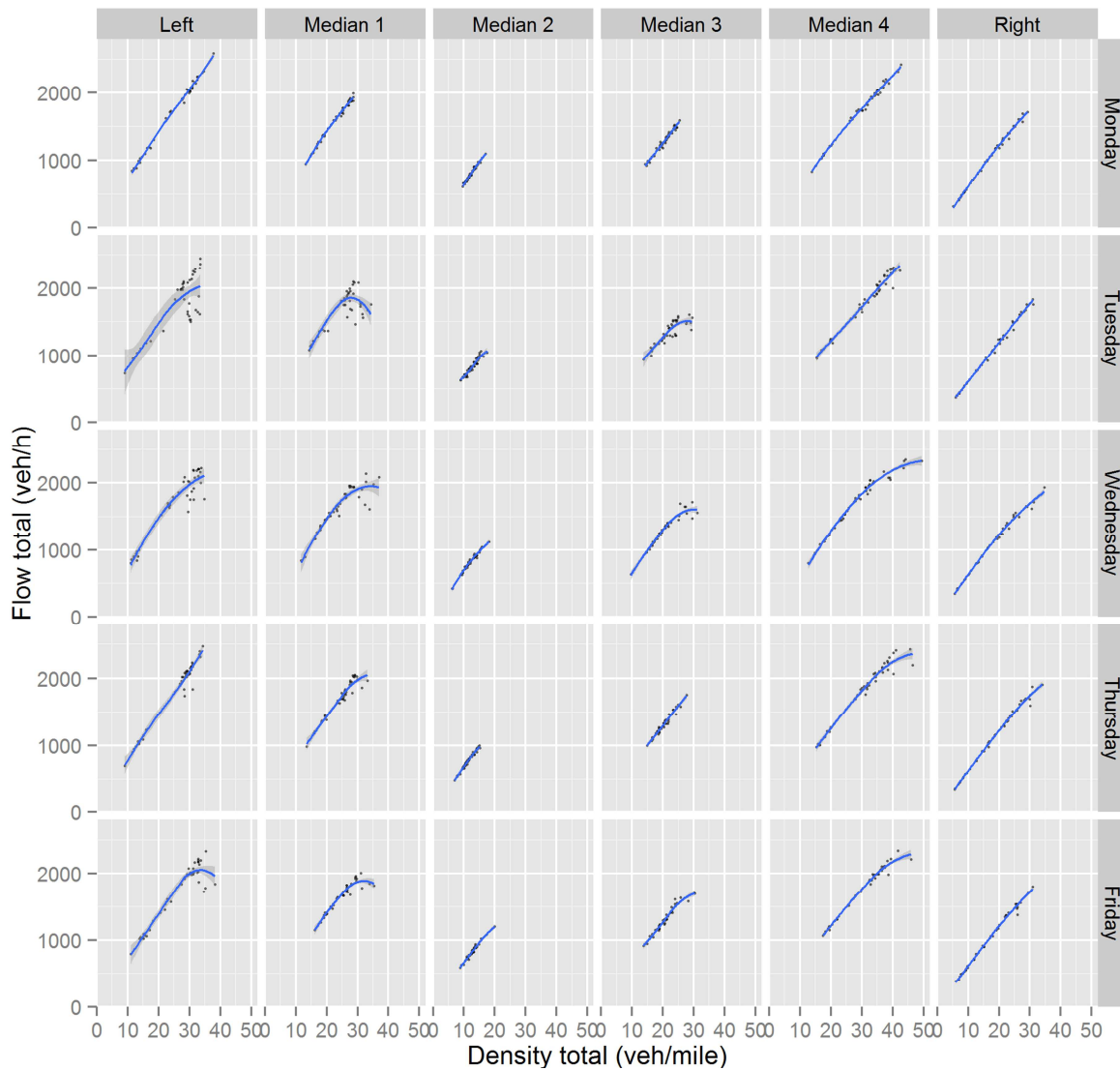


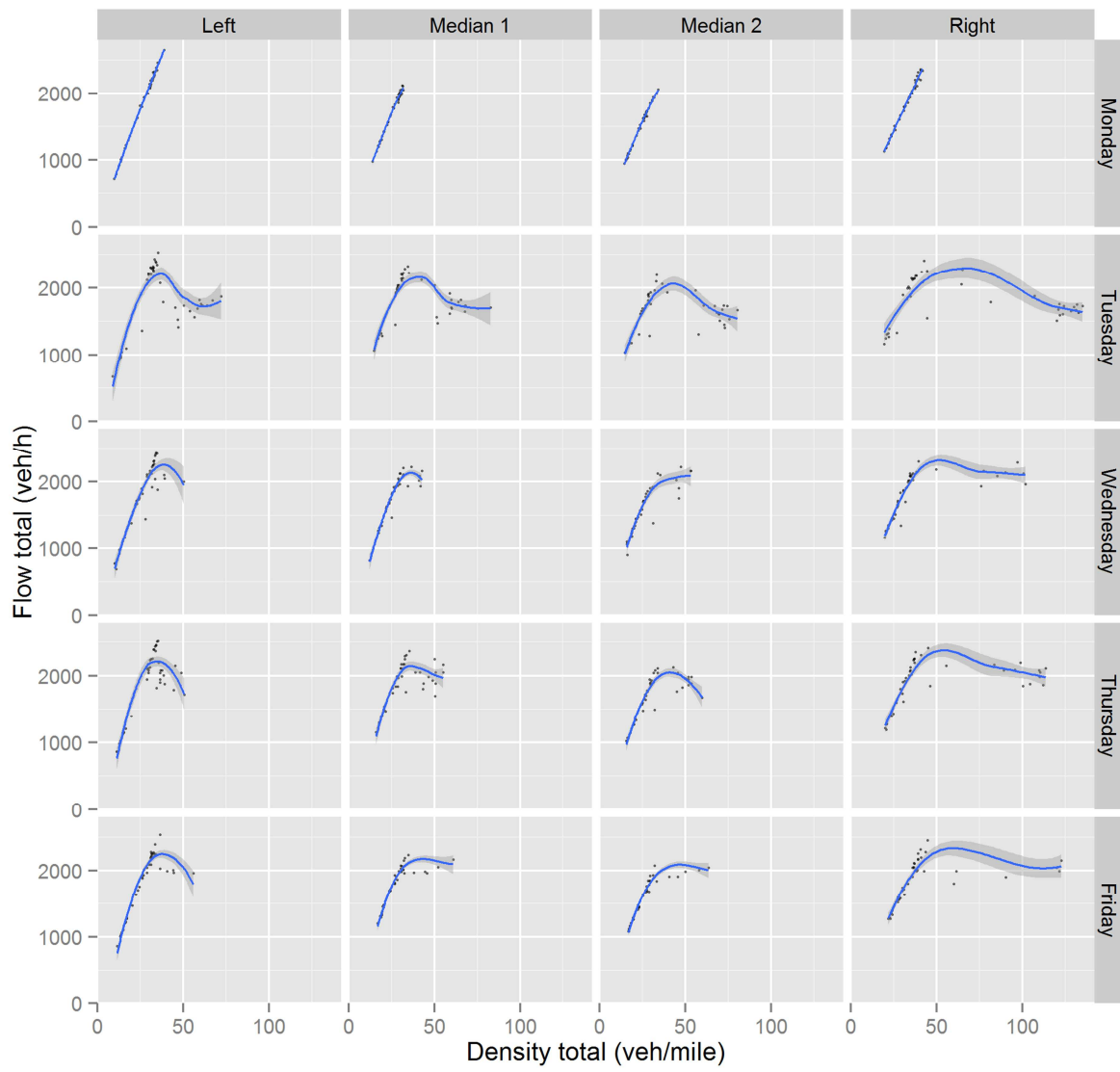
e1)



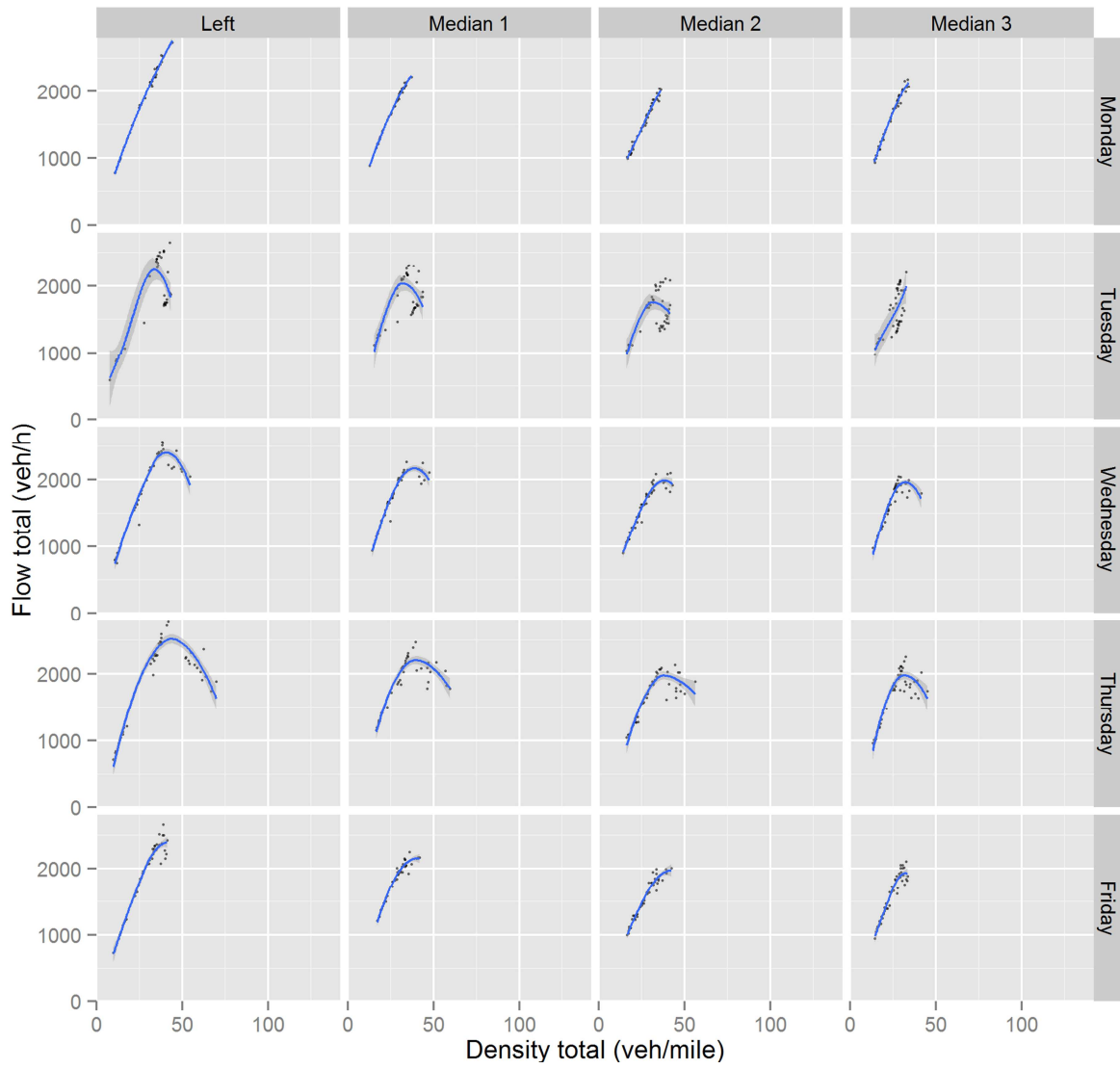
e2)

Figure A4 Diagrams of density-flow (1: per lane and 2: per direction) relationships for 5-min aggregated data during morning peak hours (6:30 – 9:55) per weekday (01-05/11/2010), fitted with loess for (in order from upstream to downstream): a) detector VDS 1117705 at mainline, 6 lanes, b) detector VDS 1114211 at mainline, 4 lanes, c) detector VDS 1117762 at off-ramp, 4 lanes, d) detector VDS 1114219 at mainline, 6 lanes and e) detector VDS 1117782 at mainline, 5 lanes.

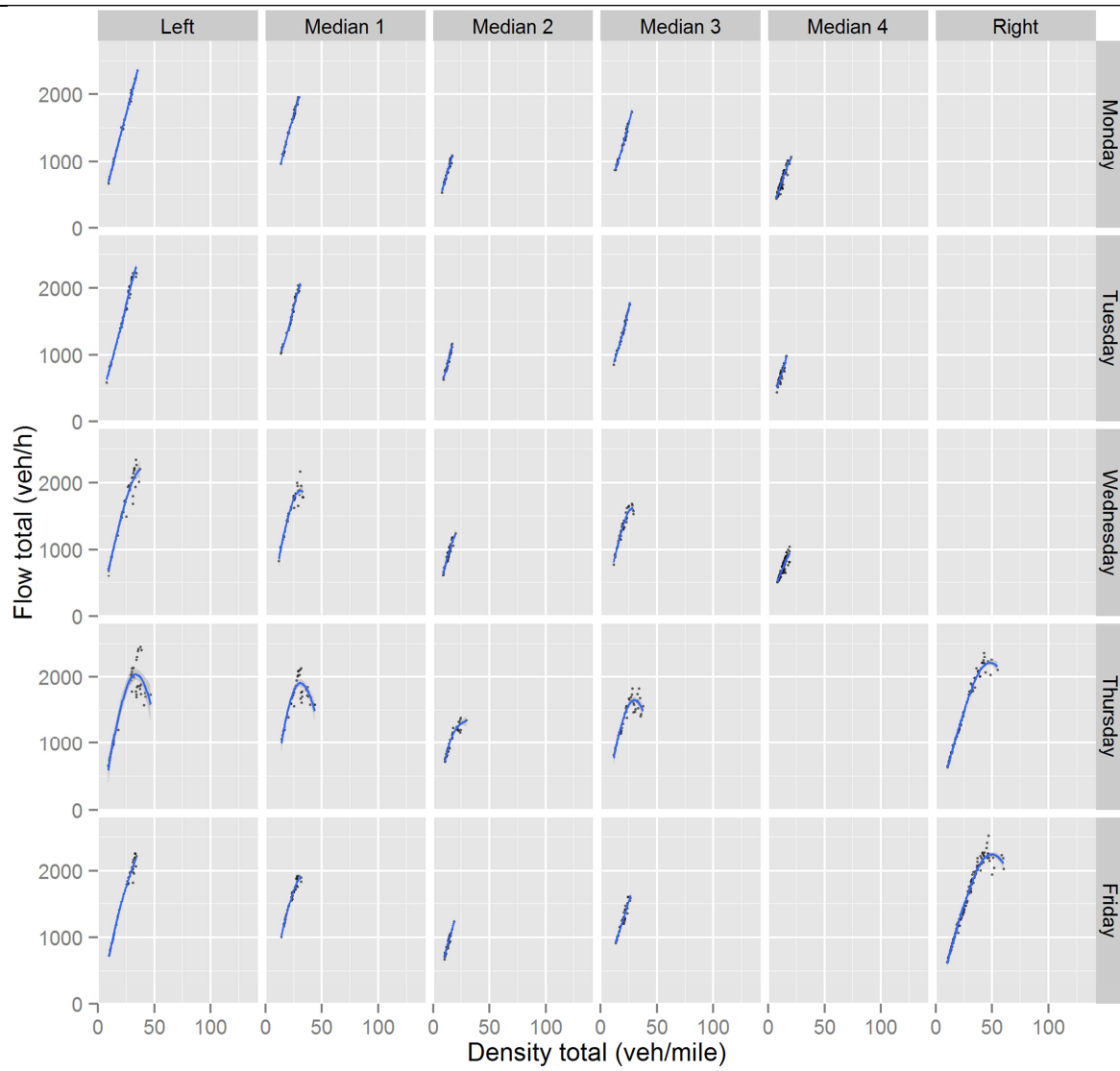
**a1)**



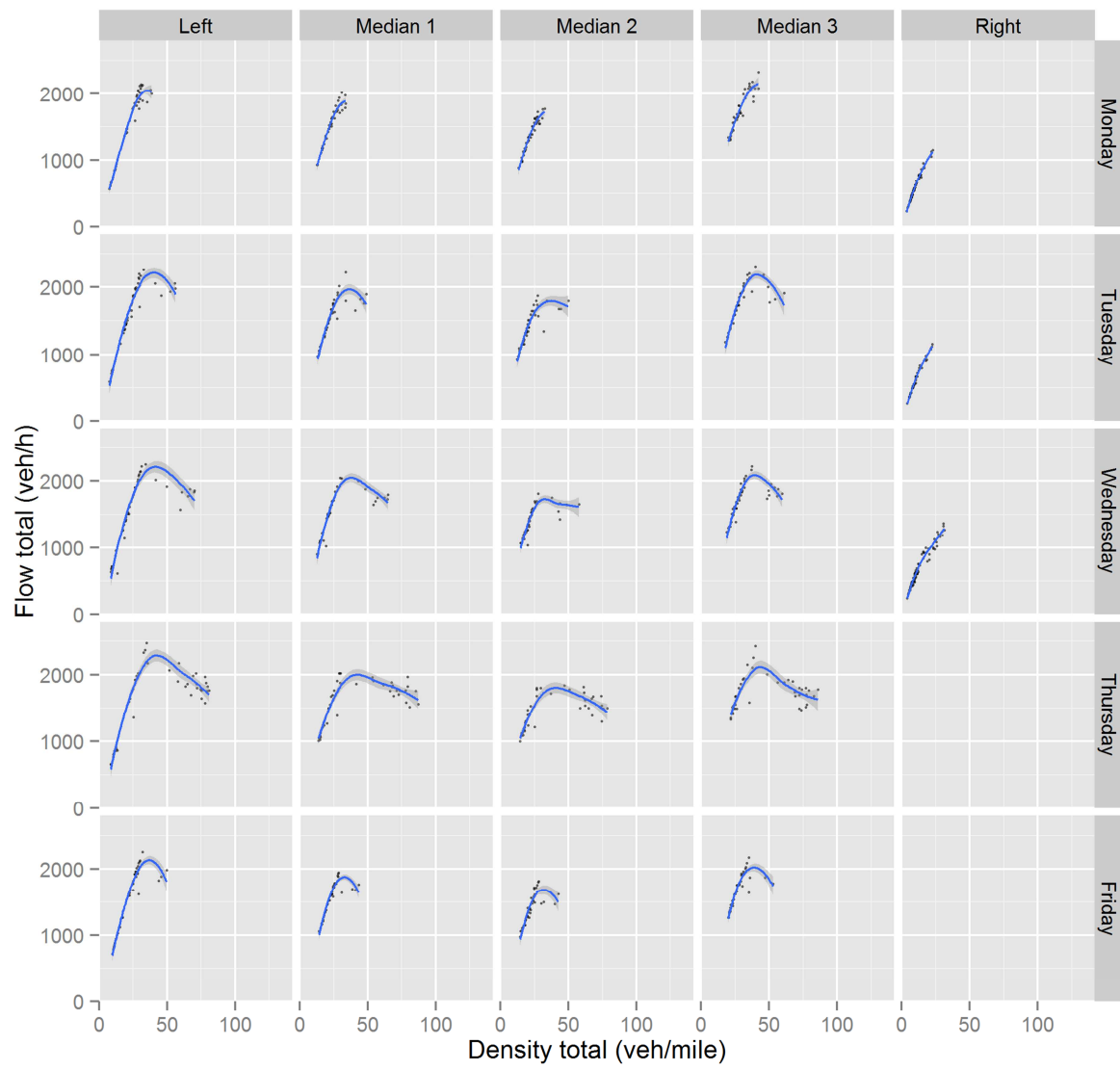
b1)



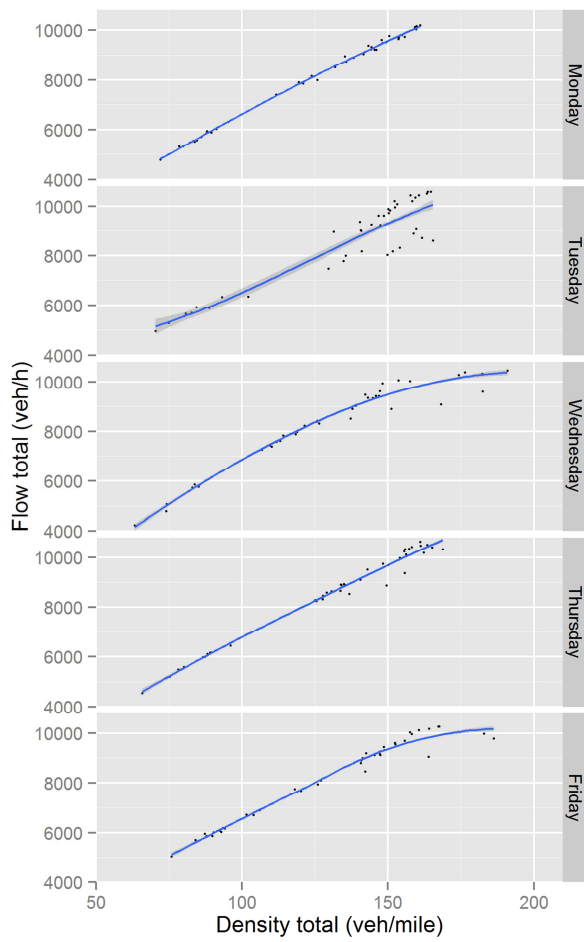
c1)



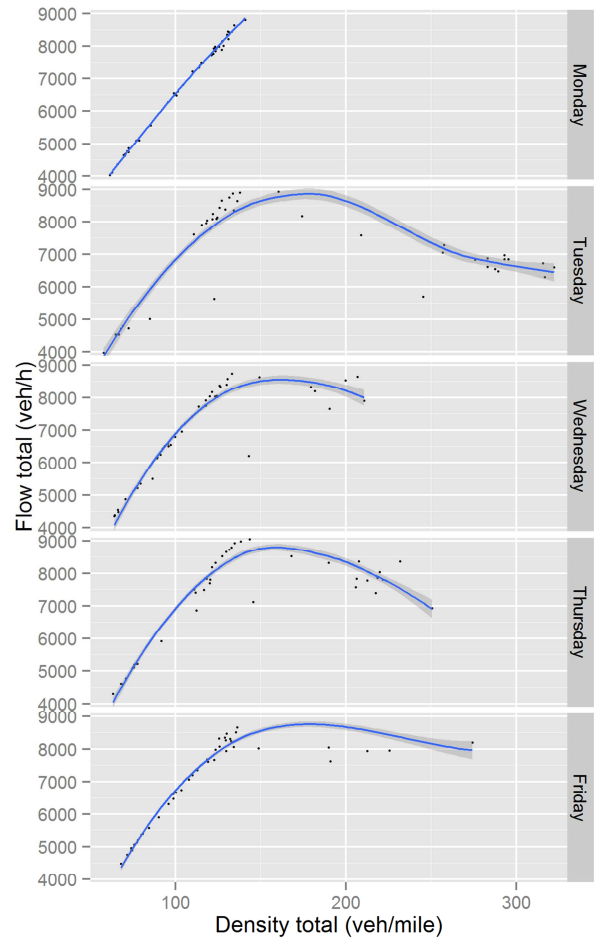
d1)



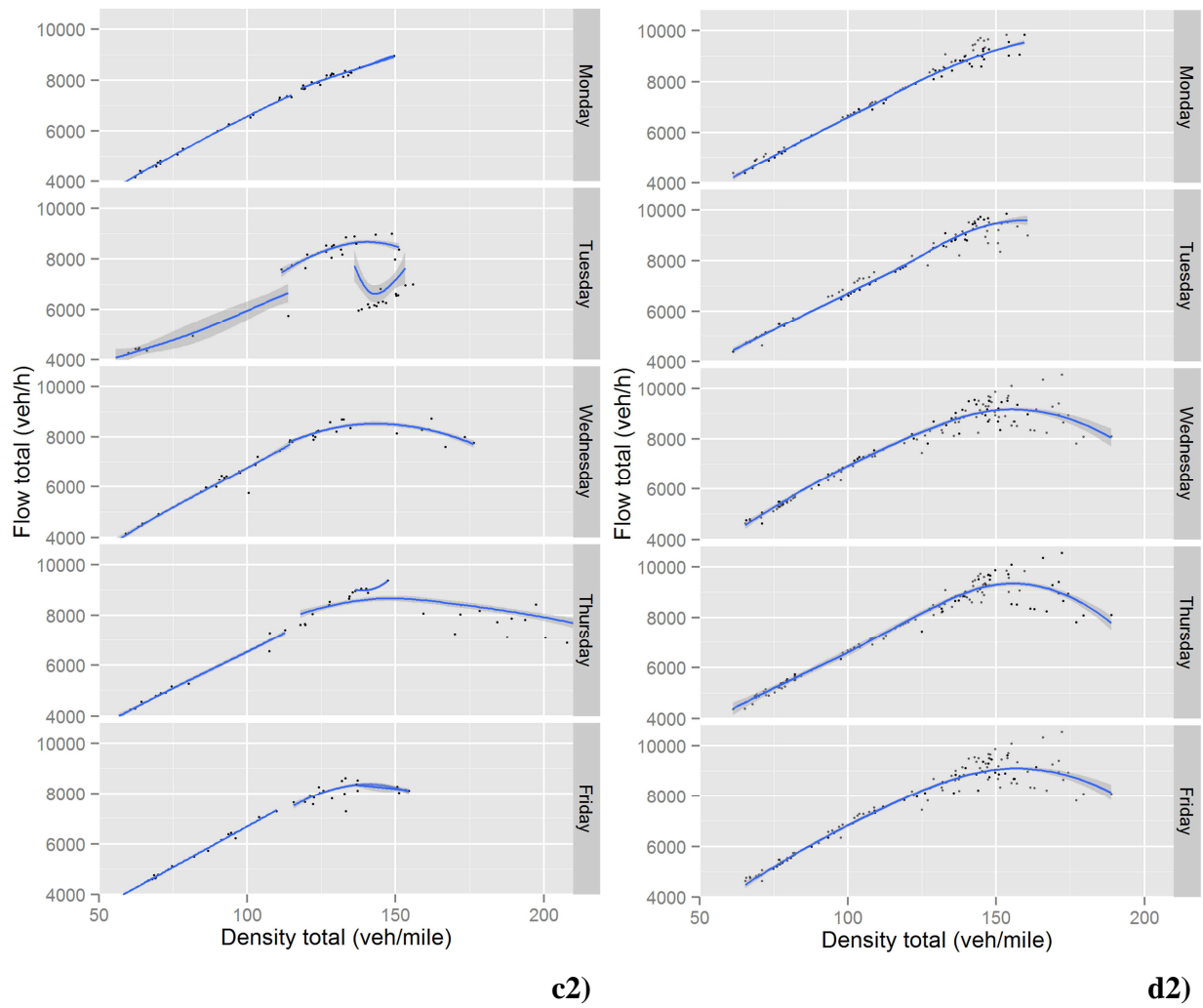
e1)

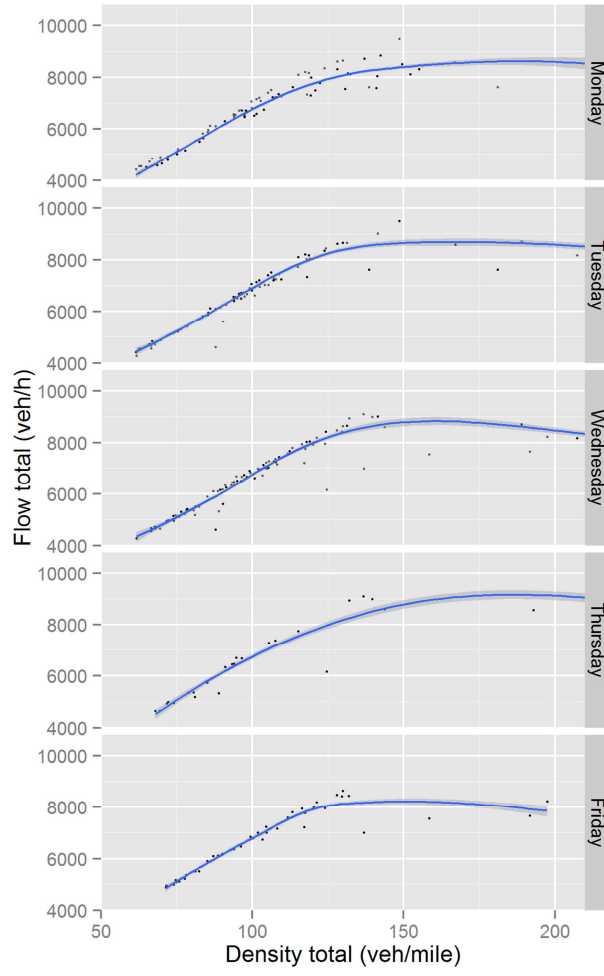


a2)



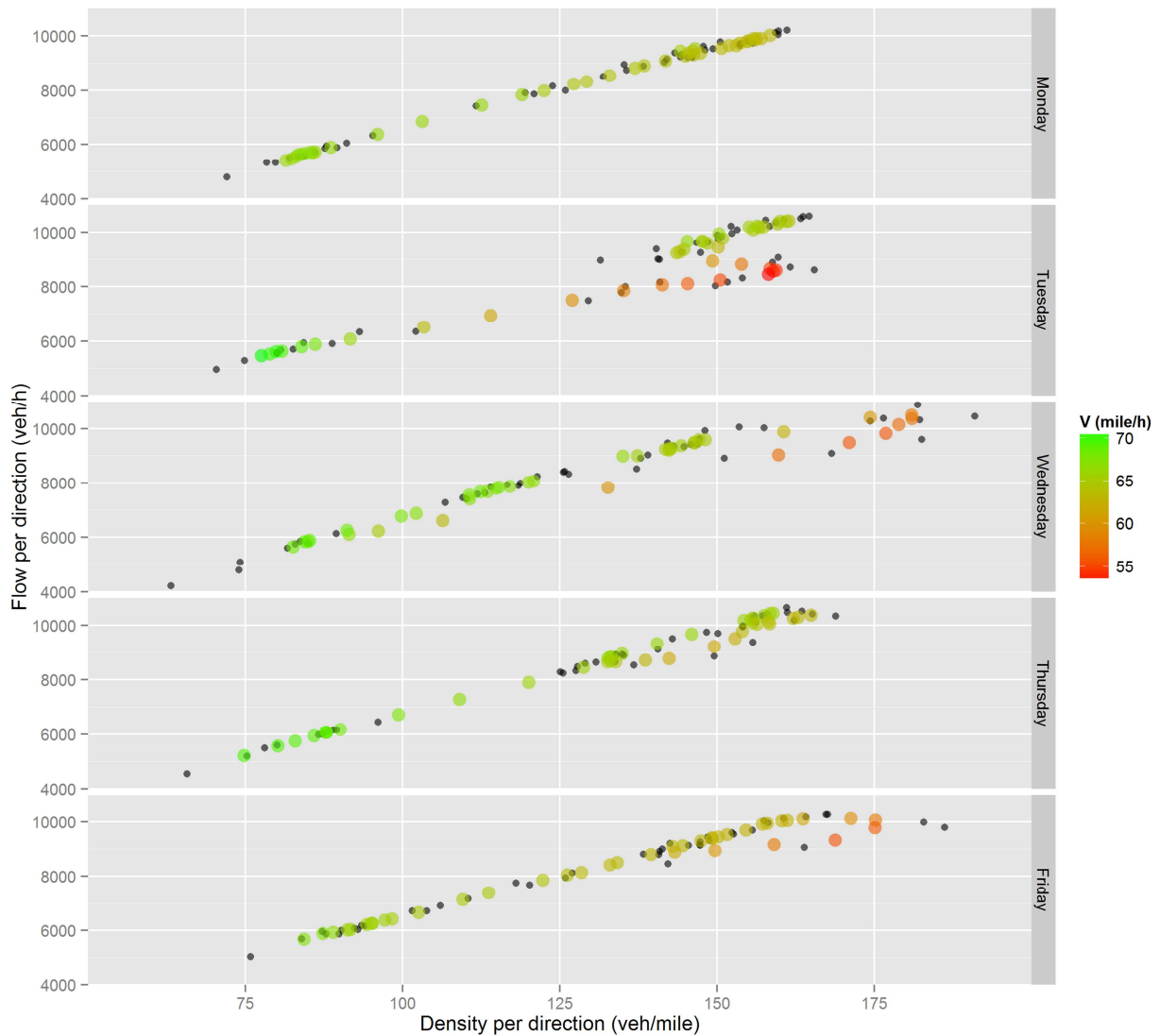
b2)

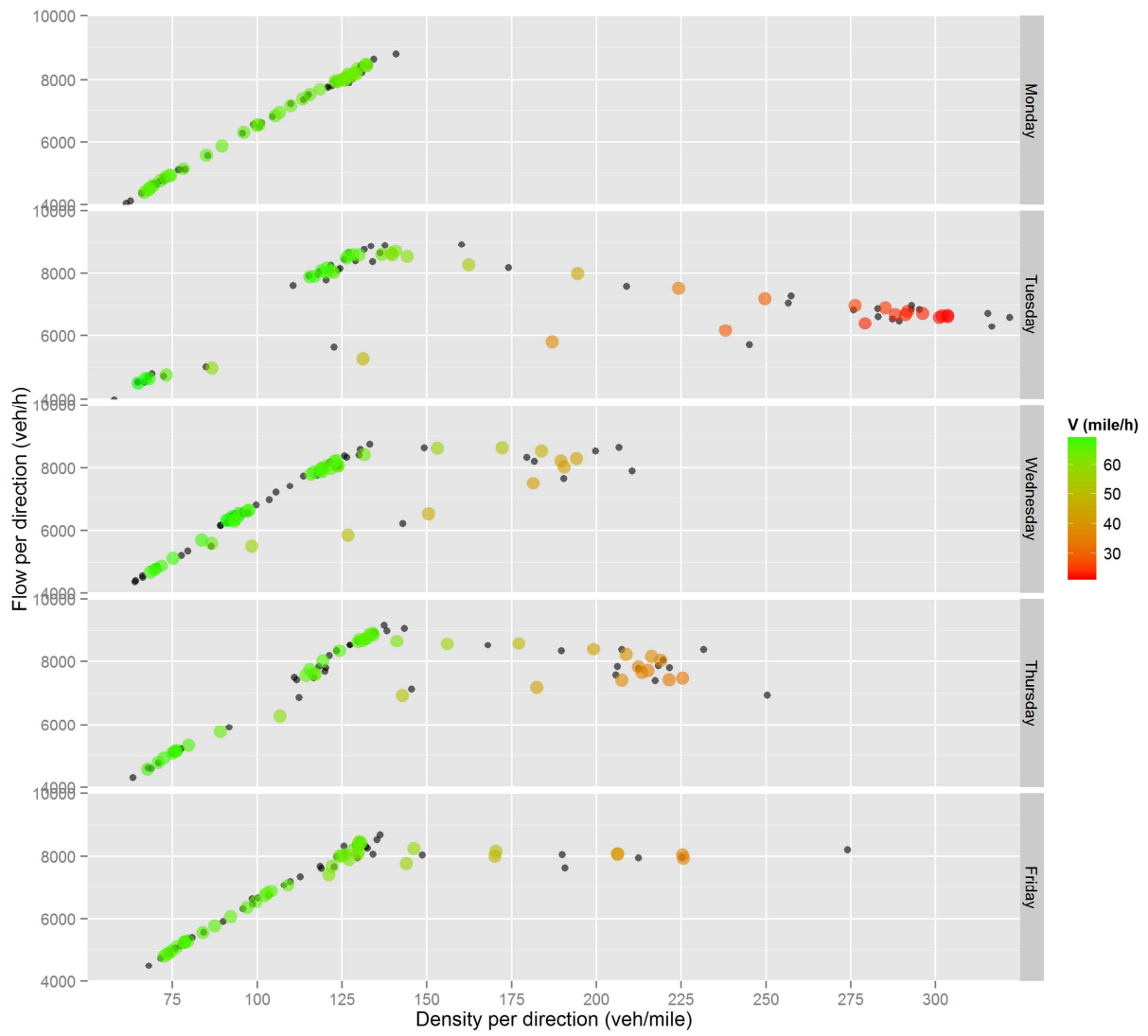




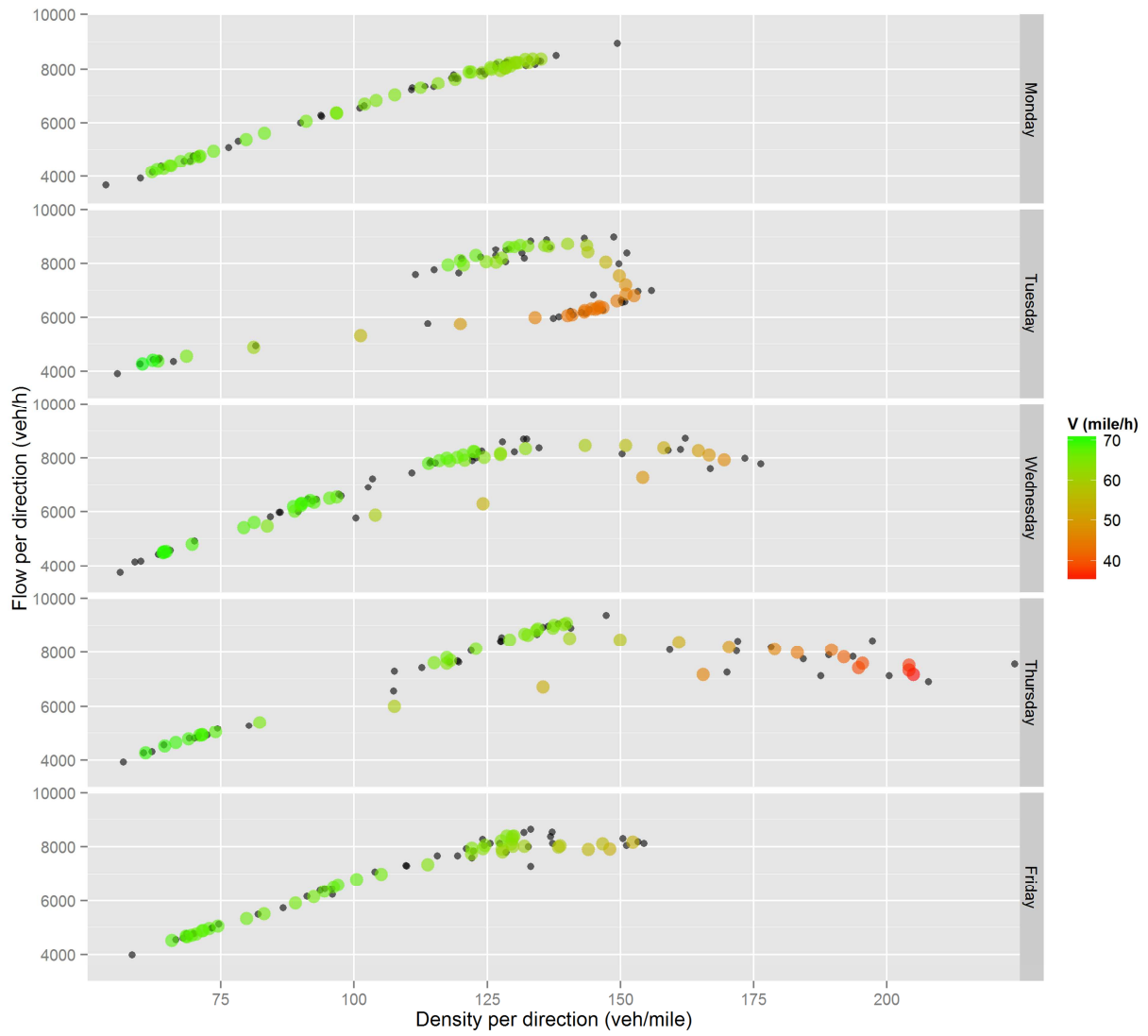
e2)

Figure A5 Diagrams of density-flow relationships for 5-min aggregated data during morning peak hours (6:30 – 9:55) per weekday (01-05/11/2010), for (in order from upstream to downstream): a) detector VDS 1117705 at mainline, 6 lanes, b) detector VDS 1114211 at mainline, 4 lanes, c) detector VDS 1117762 at off-ramp, 4 lanes, d) detector VDS 1114219 at mainline, 6 lanes and e) detector VDS 1117782 at mainline, 5 lanes. With black points are depicted the observed values of density vs. flow, and with colour the values of density vs. flow as result of a 5-min moving average every 15-min based on the levels of speed, computed with the same moving average window.

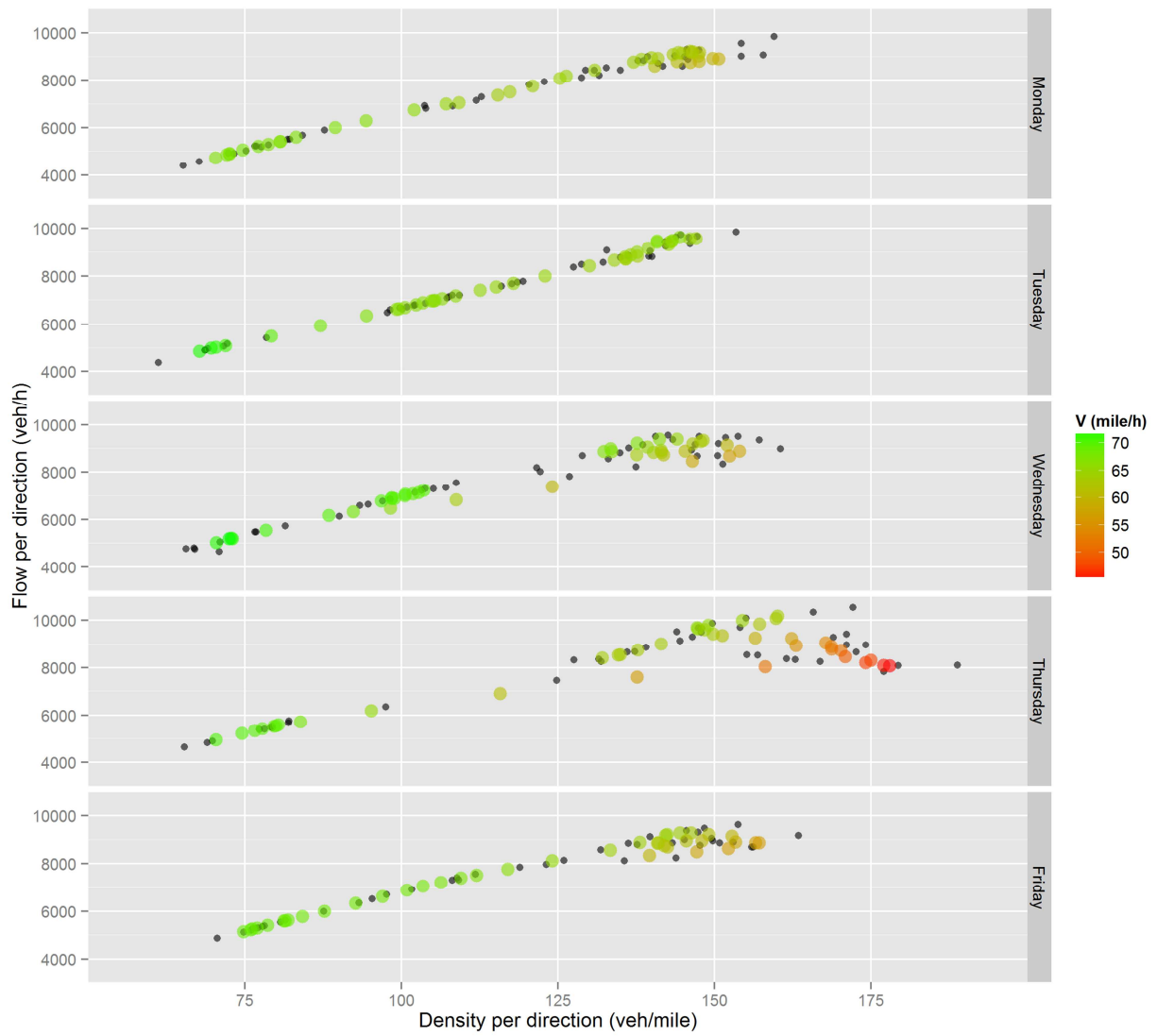
**a)**



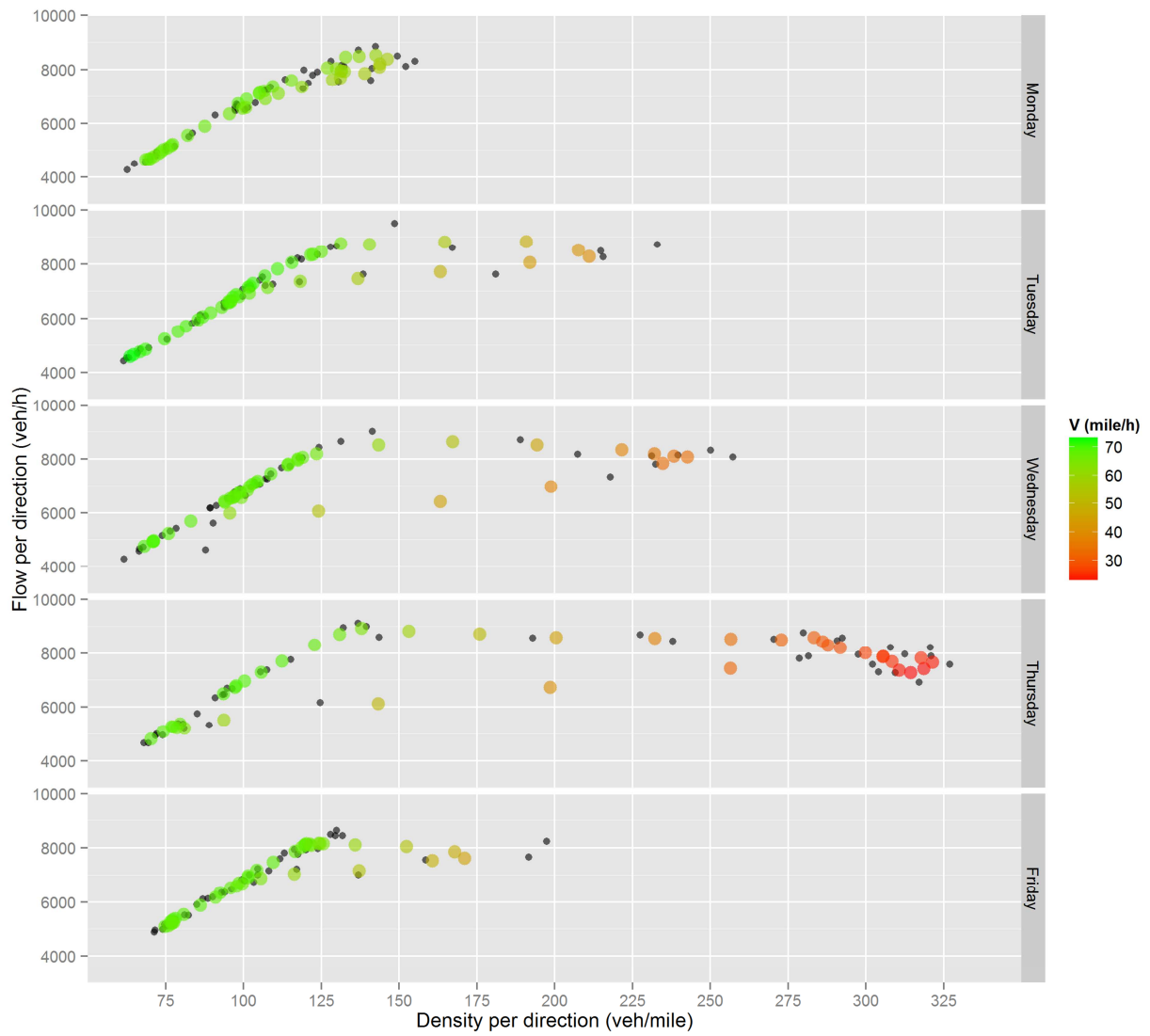
b)



c)



d)



e)